Maturation of the human B-cell receptor repertoire with age

Marie Ghraichy[1,2], Jacob D. Galson[2], Aleksandr Kovaltsuk[3], Valentin von Niederhäusern[1,2], Jana Pachlopnik Schmid[1,2], Mike Recher[4], Annaïse J Jauch[4], Enkelejda Miho[5], Dominic F. Kelly[6], Charlotte M. Deane[3], Johannes Trück[1,2*]

[1]Division of Immunology, University Children's Hospital, University of Zurich, Zurich, Switzerland

[2]Children's Research Center, University of Zurich, Zurich, Switzerland

[3]Department of Statistics, University of Oxford, Oxford, United Kingdom

[4]Immunodeficiency Laboratory, Department of Biomedicine, University and University Hospital of Basel, Basel, Switzerland

[5]University of Applied Sciences and Arts Northwestern Switzerland FHNW, Institute of Medical Engineering and Medical Informatics, Muttenz, Switzerland

[6]Oxford Vaccine Group, Department of Paediatrics, University of Oxford, Oxford, United Kingdom

[*]Corresponding author & lead contact: Johannes Trück, MD DPhil, University Children's Hospital, Steinwiesstrasse 75, 8032 Zurich, Switzerland. +41 44 266 7111; johannes.trueck@kispi.uzh.ch

Keywords

Antibody; B cells; B-cell receptor; Children; Maturation; Repertoire

Content

- Figures: 8
- Tables: -
- Supplementary Figures: 8
- Supplementary Tables: 2
- Word count manuscript: 4734
- References: 59

Funding

Swiss National Science Foundation (Ambizione-SCORE: PZ00P3_161147; PZ00P3_183777) (JT)
Gottfried und Julia Bangerter-Rhyner-Stiftung (JT)
Olga Mayenfisch Stiftung (JT)
Palatin-Stiftung (JT)
Investment fund of the University of Zurich (JT)
Swiss National Science Foundation (Professorship: PP00P3_181038) (MR)

Author contributions

JT designed and supervised the study, oversaw analyses, had full access to all the data in the study and takes responsibility for the integrity of the data and the accuracy of the data analysis. The first draft was written by JT and MG. VvN, JDG and MG processed samples and prepared sequencing libraries. MG, JDG, AK and JT performed bioinformatic analysis, revised the manuscript and approved the final version. JPS, MR, AJJ, EM, DFK and CMD contributed to manuscript revision, and approved the final version.

Competing interests

None of the authors have declared any conflict of interest related to this work.

Abstract

B cells play a central role in adaptive immune processes, mainly through the production of antibodies. The maturation of the B-cell system with age is poorly studied. We extensively investigated age-related alterations of naïve and antigen-experienced B-cell receptor (BCR) repertoires. The most significant changes were observed in the first 10 years of life, and were characterized by altered immunoglobulin gene usage and an increased frequency of mutated antibodies structurally diverging from their germline precursors. Older age was associated with an increased usage of downstream constant region genes and fewer antibodies with self-reactive properties. As mutations accumulated with age, the frequency of germline-encoded self-reactive antibodies decreased, indicating a possible beneficial role of self-reactive B-cells in the developing immune system. Our results suggest a continuous process of change through childhood across a broad range of parameters characterizing BCR repertoires and stress the importance of using well-selected, age-appropriate controls in BCR studies.

(149 words)

Introduction

B cells play a central role in physiological adaptive immune processes and exert their main effector function through production of antibodies (1). B cells also contribute to the pathogenesis of autoimmune disease via generation of auto-reactive antibodies and modulation of T-cell responses (2, 3). The heavy and light chains of the B-cell receptor (BCR, membrane-bound antibody) are generated in the bone marrow by recombining individual variable (V), diversity (D) and joining (J) gene segments through a process called VDJ recombination. Upon antigen recognition, a BCR is further diversified through rounds of somatic hypermutation (SHM) leading to affinity maturation whereby B cells with improved antigen-binding properties are selected in the germinal center. Class switch recombination (CSR) is also initiated following antigen encounter, causing a change in the constant region of the BCR and in its effector function.

Detailed characterization of B cells and their respective BCR sequences offers important information on B-cell generation and selection as well as immune competence in health and disease. High-throughput sequencing of antibody genes (Ig-seq) has become a widely used tool in human translational research (4, 5). Abnormal B-cell responses can be explored by investigating BCR repertoires from patients and comparing their characteristics to those of healthy controls. The limited data already available suggest that significant changes occur in the properties of BCR repertoires with age (6). It is therefore important to establish robust data on normal BCR repertoires within sufficiently narrow age-bands to fully understand the process of BCR maturation. This will facilitate the use of Ig-seq to understand changes of relevance to childhood disease. Given the high burden of infectious diseases in childhood and the importance of effective immune response to vaccines to prevent infection, this is an important group from which to have normative data. There are very few studies that have used Ig-seq to investigate the healthy BCR repertoire, and these studies include a limited age range of participants (7–10). In a more detailed study, Ijspeert et al. reported on the antigen-experienced (i.e. IgA and IgG) BCR repertoires of 38 healthy control (HC) samples with their ages ranging from newborn to 74 years (11). The authors found several characteristics of the studied BCR repertoire varying with age and identified patterns that are specific for isotype subclasses. However, their study was limited by the number of samples from children, the low depth of sequencing, and the small number of B-cell subsets analyzed.

We aimed to assess in detail the naïve and antigen-experienced BCR repertoires in children and young adults using isotype-resolved barcoded RNA-based Ig-seq technology and extensive bioinformatic analysis. This approach allowed us to comprehensively address the age effect on the BCR repertoire in healthy individuals and also provides a robust data set that can serve as a future reference for studying BCR repertoires in children as well as young adults with disease.

Methods

Study participants and cell isolation

Study participants were recruited with informed consent under ethical approval (KEK-ZH 2015-0555 and EKNZ 2015-187). Blood samples (5-9 mL) were collected at a single time point from 53 healthy participants aged 6 months to 50 years (**Supplementary table 1**). Peripheral blood mononuclear cells (PBMC) were isolated by centrifugation of PBS-diluted blood over Ficoll-Paque Plus (Sigma-Aldrich). Either PBMC or B cells magnetically sorted using the AutoMACS Pro cell separator and CD19+ microbeads (both Miltenyi Biotec), were lysed in RLT buffer (Qiagen), snap frozen on dry ice and then stored at -80 °C prior to use. Cells were counted using an optical microscope and an improved Neubauer chamber. The B-cell number was recorded based on actual counts or estimated using PBMC counts and either B-cell frequencies from flow cytometry performed on the same blood sample or the median percentage of age-dependent reference values (12) if the former was not available.

RNA isolation and library preparation

RNA was extracted from stored samples using the RNeasy Mini Kit (Qiagen). Reverse transcription was performed using SuperScript III/IV (Invitrogen) according to the manufacturer's instructions and constant region primers that included 14 nt unique molecular identifiers (UMI), and partial p7 adaptors. Two reverse transcription reactions were carried out for each sample: one with a mix of IgM and IgD-specific reverse primers and another with a mix of IgA, IgG, and IgE-specific reverse primers. From 6 samples, one mix with all C region primers were used in a single reaction. Primer sequences with concentrations are included in **Supplementary table 2**. BCR heavy chain rearrangements were amplified in a two-round multiplex PCR; the first round using a mix of V family specific forward primers with partial p5 adaptors, and the second round to complete the adaptor sequences. PCR conditions for the first round were 95 °C for 5 min, either 8 cycles (IgD/IgM) or 12 cycles (IgA/E/G) of 98 °C for 20s, 60 °C for 45s and 72 °C for 1 min, and 72 °C for 5 minutes. The PCR conditions for the second round were 95 °C for 5 min, 22 cycles of 98 °C for 20s, 69 °C for 20s and 72 °C for 15 sec, and 72 °C for 5 minutes. PCR amplicons were gel-extracted, purified and quantified using the Illumina qPCR library quantification protocol. Individual libraries were normalized based on concentration and then multiplexed in batches of 24 for sequencing on the Illumina MiSeq platform (2 x 300 bp paired-end chemistry). Compared with short-read sequencing protocols, long read RNA sequencing on the Illumina MiSeq instrument results in less deep sequencing. However, long read sequencing provides information on the entire VDJ sequence and the constant region of the BCR allowing for accurate distinction between isotypes and subclasses.

Sequence processing, annotation and somatic hypermutation

Samples were demultiplexed via their Illumina indices, and initially processed using the Immcantation toolkit (13, 14). Briefly, raw fastq files were filtered based on a quality score threshold of 20. Paired reads were joined if they had a minimum length of 10 nt, maximum error rate of 0.3 and a significance threshold of 0.0001. Reads with identical UMI (i.e. originating from the same mRNA molecule) were collapsed to a consensus sequence. Reads with identical full-length sequence and identical constant primer but differing UMI were further collapsed resulting in a dataset containing a set of unique sequences per sample and isotype. Sequences were then submitted to IgBlast (15) for VDJ assignment and sequence annotation, and unproductive sequences removed. Constant region sequences were mapped to germline using Stampy (16) for isotype (subclass) annotation, and only sequences with a defined constant region were kept for further analysis. The number and type of V gene mutations was calculated using the shazam R package (14). Levels of somatic hypermutation (SHM) were determined by calculating V gene mutations in individual sequences, and mean values were calculated across samples and cell subsets.

Sequence clustering, clonal lineages and antigen-driven selection

Sequences were independently clustered for each sample to group together those arising from clonally related B cells. The clustering required identical V and J segment use, identical complementary-determining region (CDR) 3 length, and allowing a 1 in 15 nucleotides mismatch in the CDR3 as previously determined (7). Lineages were constructed from clusters using the alakazam R package (17). To account for read depth variation, lineage trees were constructed on subsamples of the original data. Specifically, we randomly sampled 25'609 sequences (corresponding to the lowest number of reads available for a sample) from every HC sample. For calculation of selection pressure of samples, individual sequences within clusters are not independent events, so an effective representative sequence of each clonal group was determined using the default settings of shazam. Selection pressure was calculated using BASELINe (18) implemented within shazam. The statistical framework used to test for selection was CDR_R / (CDR_R + CDR_S), which normalizes for the observed increase in the total number of mutations with age. The replacement/silent (R/S) mutation ratio was measured separately in framework regions (FWRs) and CDRs. In sequences with replacement but no silent mutations, the number of silent mutations was set to 1.

From Sequence to Structure

The SAAB+ pipeline was employed to annotate BCR repertoires with structural information (19). Briefly, BCR repertoires were numbered with the IMGT scheme (20) and filtered for structural viability using 'ANARCI parsing' (21) as per the first steps of the ABOSS algorithm (22). Sequences were filtered out that (i) could not be aligned to the human Hidden Markov Model (HMM) profile of an IMGT germline (ii) had a J gene sequence identity of less than 50% to a human IMGT germline or (iii) contained non-amino acid entries in CDRs. Since the primer masking step in pRESTO (13) can remove the first framework region and positions 127 and 128 of some sequences, ANARCI parsing was customized to account for these exceptions. To retain as many sequences as possible for structural annotation, we substituted undetermined residues in the framework region with the residues from their respective parent germline genes.

To annotate the numbered sequences with canonical loop class information, SAAB+ employs SCALOP (23) with the IMGT CDR definition (20). The expected coverage of canonical loop class sequences with SCALOP is 93%, where 89% of predicted templates will have root-mean-square deviation (RMSD) values for the backbone atoms within 1.5 Å of the correct structure. The SCALOP database dated July 2018 was used in this study.

SAAB+ employs FREAD (24) to annotate CDR-H3 loops with the Protein Data Bank (PDB) code (25) of the closest crystallographically-solved CDR-H3 structure (template). Only CDR-H3 sequences with loop lengths between 5 and 16 were investigated. The expected average RMSD of CDR-H3 template prediction for the human BCR repertoire data is 2.8 Å, with an expected coverage of 48% (19). PDB templates within a 0.6 Å RMSD radius were clustered together (19), reducing 2'943 PDB templates to 1'169 CDR-H3 PDB clusters.

Statistical analysis and graphing

Statistical analysis and plotting were performed using R (26); all plots were produced using the ggplot2 and ggpubr packages (27, 28). Heatmaps were visualized using the ComplexHeatmap R package (29). PCA plots were created using the R package factoextra (30). In cases where a model was fitted to the data, the R squared of the model and the p value of the chi-squared goodness-of-fit test are shown in the bottom right of the graphs. Other specific tests used are detailed in the figure legends.

Classification of sequences into cell subsets using isotype and number of mutations

Using constant region annotation and mutation number, individual sequences were grouped into biologically different subsets based on known B-cell subpopulations. Based on the frequency distribution of mutations for IgD and IgM sequences, those with up to 2 nt mutations across the

entire V gene were considered “unmutated” (naïve) to account for allelic variance (31) and remaining PCR and sequencing bias (**Supplementary figure 1**). All class-switched sequences were defined as antigen-experienced irrespective of their V gene mutation count. Because of very low sequence numbers, IgE and IgG4 transcripts were excluded from most analysis. The number of sequences of the different subsets among total transcripts by individual are found in **Supplementary table 1**.

Data availability

Raw sequence data used for analysis in this study are available at the NCBI Sequencing Read Archive (www.ncbi.nlm.nih.gov/sra) under BioProject number PRJNA527941 including metadata meeting MiAIRR standards (32). The processed and annotated final dataset is available in Zenodo (https://doi.org/10.5281/zenodo.3585046) along with the protocol describing the exact processing steps with the software tools and version numbers.

Results

We obtained 78'702'939 raw sequences from samples of 53 healthy study participants. Processing, filtering and collapsing resulted in a final dataset of 8'341'669 unique BCR sequences used for downstream analysis. The numbers of unique sequences were significantly reduced after UMI-based collapsing resulting in a correlation with the B-cell numbers per sample (**Supplementary figure 2**).

V family and J gene usages change with age

Although previous work has observed common patterns of gene segment usage and has suggested a strong dependence on an individual's germline genetic background (33, 34), the relative contributions to variance from age remained unclear. Proportions of sequences assigned to the different V gene families and J genes were calculated for each sample and B-cell subset. The overall distribution of V family and J gene usage were different in older individuals compared with younger age groups. In particular, frequencies of V1 family sequences significantly decreased with age in naïve and mutated IgD and IgM sequences. This decrease was also observed in IgG and IgA antibody although with higher individual variation in older age groups (**Figure 1A**). No clear pattern was found in the usage of the other V families by age (**Supplementary figure 3A**). Such changes in V1 family genes were due to age-related alterations in several V genes, particularly VH1-8 (**Supplementary figure 5**).

There were also changes in the overall J gene usage over the first 10 years of life marked by a significant decrease in the frequencies of sequences assigned to J6 in IgG antibody (**Figure 1B**). Frequencies of the other J genes by age group are shown in **Supplementary figure 3B**. In line with previous work (35, 36), we find that BCR sequences with rearranged J6 gene have longer junctions (**Supplementary figure 3C**). Along with a declining J6 usage with age, a significant decrease in junction length was observed in IgG subsets of older individuals (**Figure 1C**). However, even within IgG J6 antibody, junction length significantly decreased with age indicating that shorter junctions in older individuals are not solely the result of altered J gene usage (**Supplementary figure 4**).

Somatic hypermutation exponentially increases in the first 10 years of life

There was a significant increase in SHM in all antigen-experienced subsets with age, which was most prominent in the first 10 years of life (**Figure 2A**). Substantial changes in mutation counts were found in all IgA and IgG subsets with exponential increases in children under 10 years and more linear progression between 10 and 50 years. IgM memory showed the smallest change of all subsets with some increase in children and a plateau from the 2nd decade while there was no age-dependent change for IgD memory antibody. However, the proportion of mutated IgM antibody per sample increased from 0.1 in 0-3 year olds to an average of 0.4 in older individuals (**Figure 2B**). An age-related increase in the proportion of mutated sequences was also seen for IgA and IgG although at a higher level (**Figure 2B**).

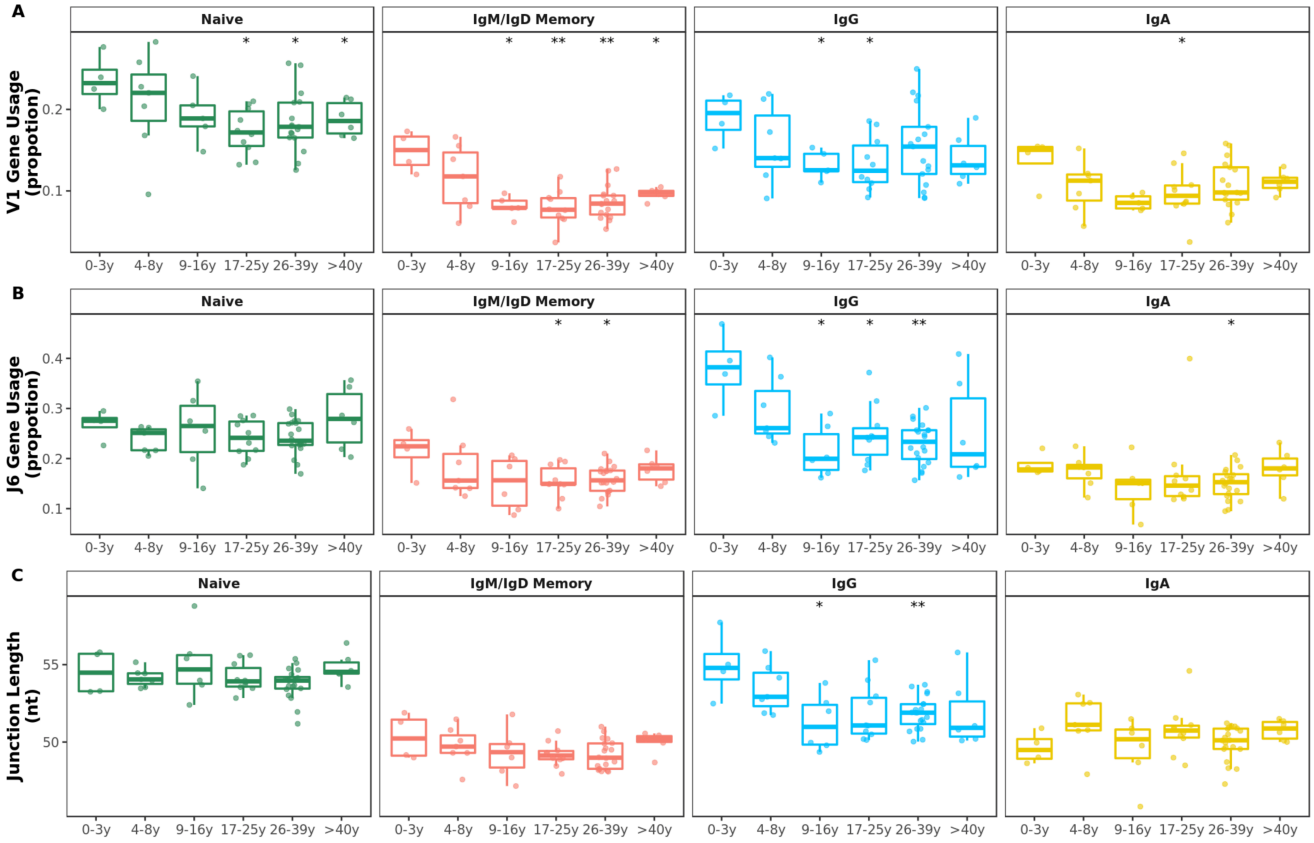

Figure 1: V family and J gene usage changes in early childhood. *A* V1 family usage was significantly reduced in older compared with younger individuals in all BCR repertoires. *B* J6 gene usage significantly decreased during the first 10 years of life mostly in IgG subsets. *C* Mean junction length significantly decreased in the first 10 years of life exclusively in IgG subsets. Comparison of each age group to the 0-3y group was performed using the Wilcoxon test. *p<0.05, **p<0.01

Sequences with predicted antibody structures diverging from germline increase with age

Crystallographic studies have shown that antibody CDR-H1 and CDR-H2 loops can adopt a very limited number of structural conformations, known as canonical loop classes (37, 38). These canonical classes are considered to be separate and distinct structures of the CDRs and can be rapidly and accurately annotated by SCALOP (23). The proportion of sequences in which either CDR-H1 and CDR-H2 had switched from the canonical class of their germline increased with age for most antigen-experienced subsets, similar to the increasing mutation number with age (**Figure 2C**).

Structures of CDR3 were predicted by mapping sequences to antibody structures in the PDB and annotated with a PDB code identifier. The proportion of every PDB cluster within individual and repertoire was calculated and normalized to zero mean and unit variance across individuals. PDB cluster usages were similar across individuals and age with a small number of positive outliers (frequent usage) that were private to each individual (**Supplementary figure 6**).

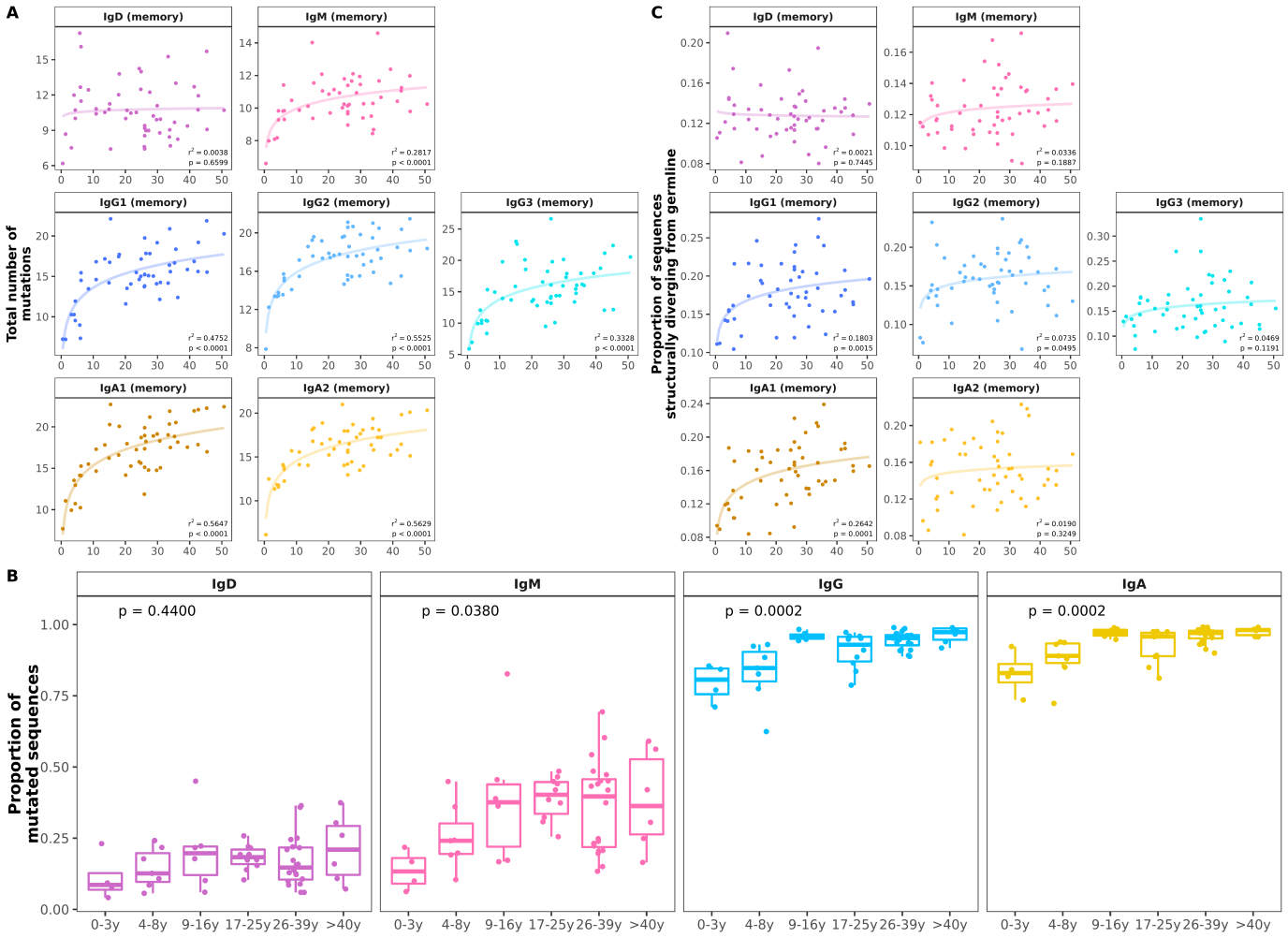

Figure 2: Age-related changes in somatic hypermutation and predicted antibody structure. *A* Mean number of V gene mutations by individual and B-cell subset with fitted logarithmic curves. Somatic hypermutation increased mainly in the first 10 years of life with some differences between cell subsets. *B* The proportion of memory IgD and memory IgM out of all IgD/IgM antibody and the proportion of mutated IgG and IgA antibody within repertoires showed significant increases in the first 10 years of life. *C* The proportion of sequences structurally different from germline increased in early childhood in all B-cell subsets. Statistical differences between groups were tested using the Kruskal-Wallis test.

Structural but not sequence clusters are commonly shared between individuals

For each of the 53 individuals in this study, we calculated the frequency of sequence clusters (i.e. clonally related sequences) that are unique to the individual, the frequency of clusters that are shared with two, three or more subjects. Overlap with n subjects was quantified as the number of clusters shared with only n individuals divided by the total number of clusters in an individual's repertoire. We found that on average, 84.1% of clusters were unique to the individual, while 2.5%, 0.2%, 0.04% and 0.02% of clusters were shared with 2, 10, 25 and 45 or more other individuals, respectively (**Figure 3A**). Sharing of structural clusters, however, was much more frequent with the majority of clusters (57%) shared by all 53 individuals and on average only 0.03% of clusters unique to the individual (**Figure 3B**). Neither sequence nor structural cluster sharing showed age-related changes.

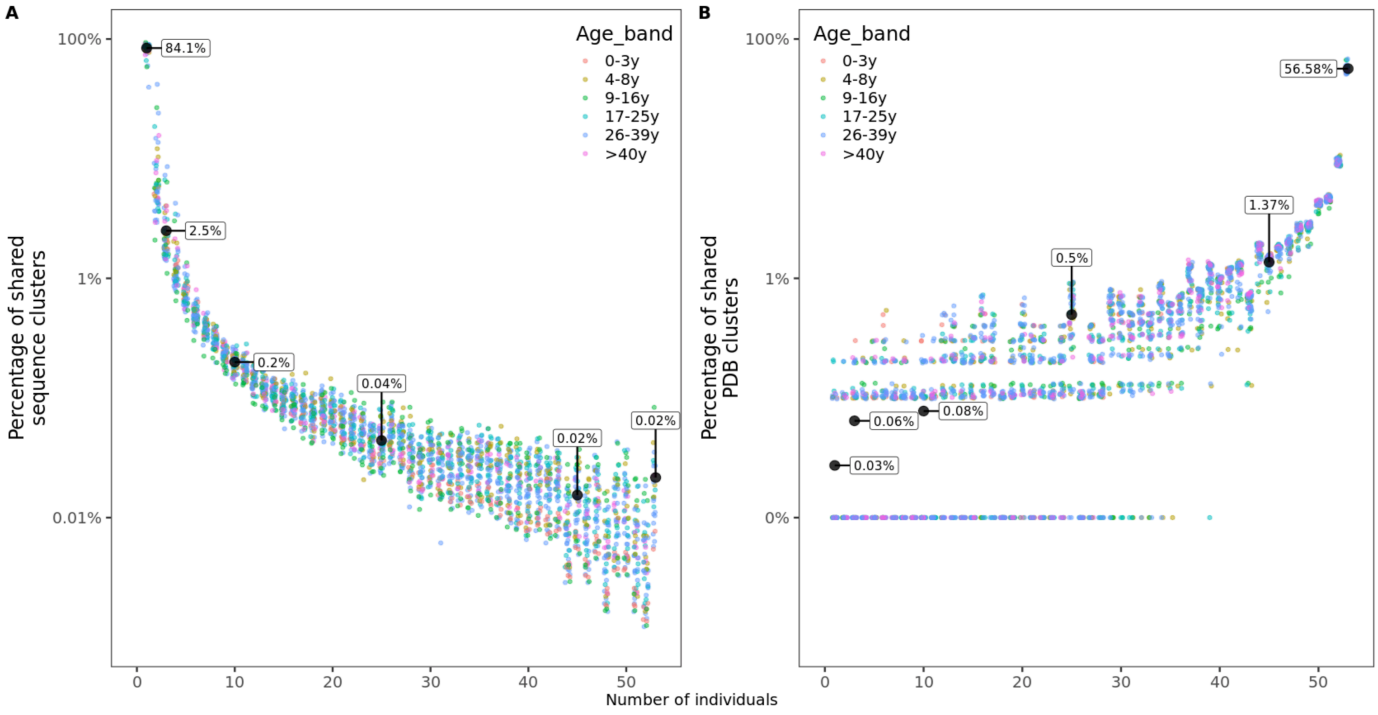

Figure 3: Sharing of sequence and structural clusters among the 53 healthy participants of different ages. *A* Percentage of sequence clusters shared by n individuals. *B* Percentage of structural clusters shared by n individuals. For structural clusters, zeros were replaced by 0.01% to be displayed on a logarithmic scale but labeled as 0%.

Older individuals display more mature clonal lineages and antibody with antigen-driven selection

Lineage trees were constructed from clusters of clonally related sequences and used to determine the evolutionary relationship within clusters (**Figure 4A**). The mean trunk length, representing the distance between the most recent common ancestor and germline sequence as a measure of the maturity of a lineage (39), greatly increased with age (**Figure 4B**). There was no relationship between age and the Gini index, which predicts whether lineages are dominated by a single clone (high index) or has a broad branching structure (low index) (**Figure 4C**). To account for differences in read depth, these characteristics were calculated on subsampled data so that the numbers of sequences were similar between individuals.

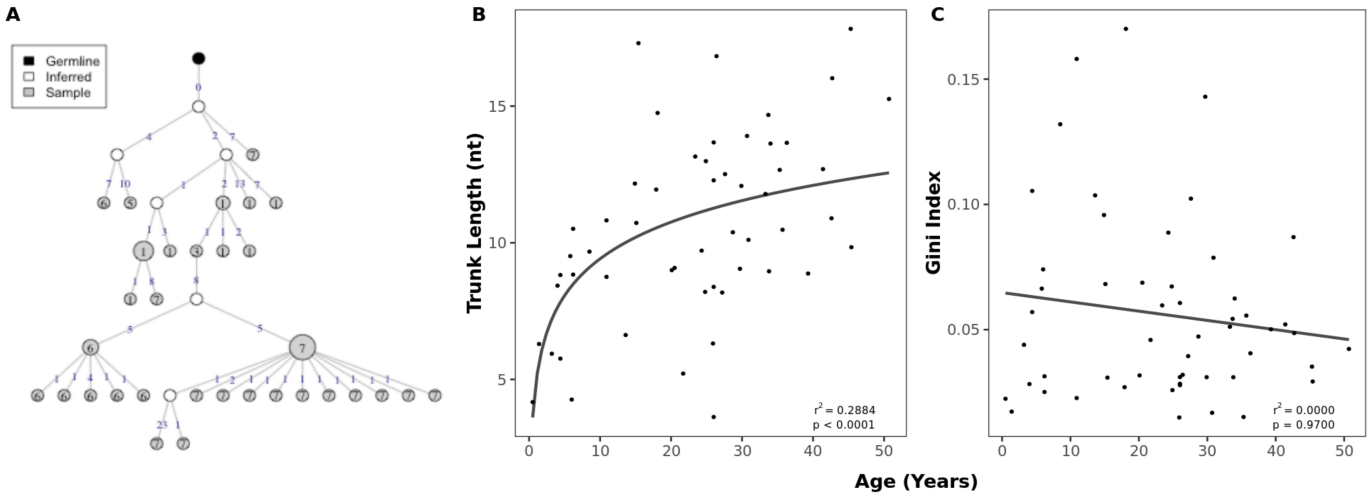

Figure 4: Age-related changes in clonal expansions. *A* Example lineage tree with each node representing a sequence and the size of the node indicating the number of identical sequences. The number of mutations between the sequences (nodes) is shown on top of the connecting lines. *B* Correlation between age and mean trunk length with a fitted logarithmic curve. *C* Correlation between mean Gini index and age with a fitted linear model.

Insights into the process of antigen-driven selection can be gained by analyzing the mutational pattern in antigen-experienced repertoires. The R/S ratio in CDRs showed a marked increase in all antigen-experienced subsets between 0 and 10 years of life (**Figure 5A**). In samples from study participants older than 10 years, the R/S ratio was largely constant with values of around 3-3.5 in all B-cell subsets. In contrast, the R/S ratio was less variable and lower in FWRs compared with CDRs and no association with age was found (**Supplementary figure 7**). Next, we determined selection pressure using a Bayesian estimation of antigen-driven selection (BASELINe), which calculates selection by comparing the observed mutations to expected mutations derived from an underlying SHM targeting model (18). In CDRs, there was a general trend towards an age-associated decrease in selection strength for IgA and IgG antibody whereas this was constant across age for IgD or IgM sequences (**Figure 5B**). The statistical framework used to test for selection was CDR_R / (CDR_R + CDR_S), which normalizes for the observed increase in the total number of mutations with age.

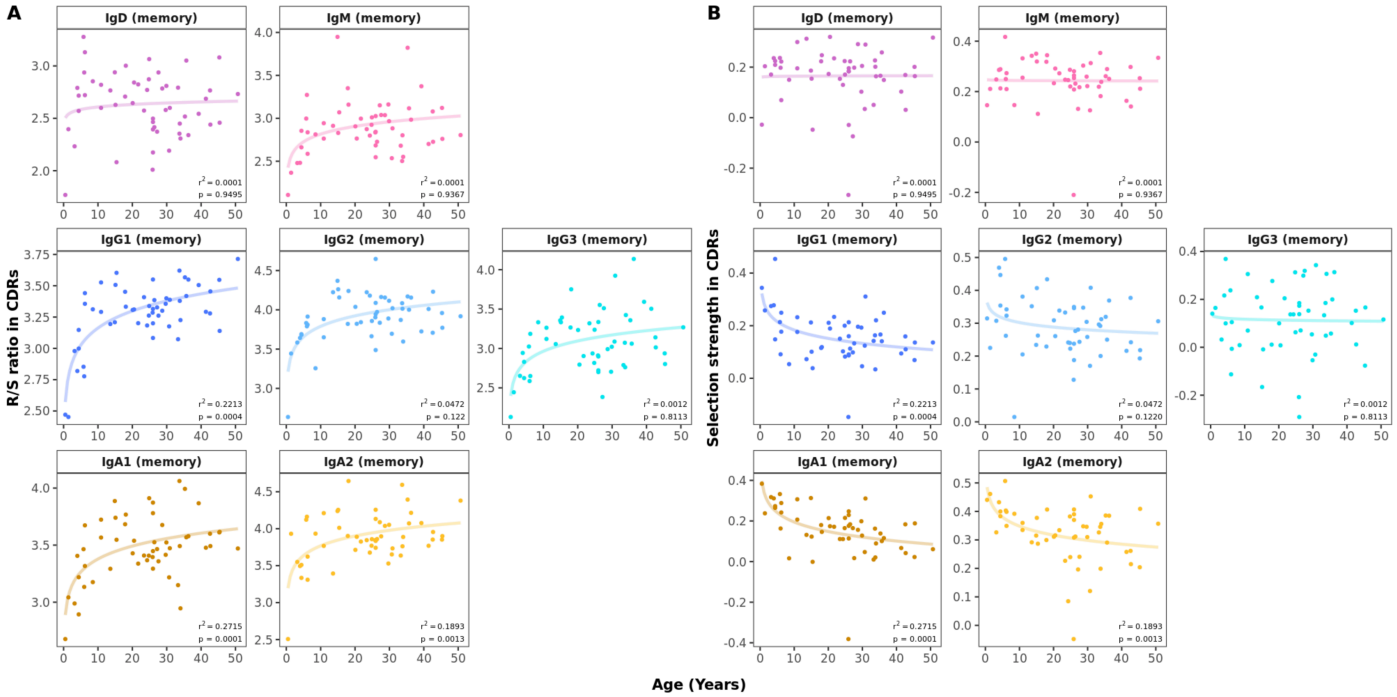

Figure 5: Age-related changes in antigen-driven selection. A) Mean R/S ratio in V gene CDRs as a measure of selection pressure showed an increase in early childhood in all B-cell subsets. For sequences with replacement but no silent mutations, the number of silent mutations was set to 1. **B)** Mean selection strength in CDRs calculated using BASELINe decreases with age in class switched subsets.

Usage of IgG2 and IgA2 subclasses increase with age

Subclass usages were calculated within IgA and IgG repertoires to explore age-dependent class-switching patterns. In most age groups, IgG1 sequences were the most commonly detected, followed by IgG2, IgG3, and IgG4 sequences. However, the proportion of IgG2 sequences increased with age (p=0.0140, Kruskal-Wallis by age group) at the expense of lower usage of IgG1 (p=0.0086, Kruskal-Wallis) and IgG3 (p=0.1900, Kruskal-Wallis) sequences in older individuals. Similarly, IgA1 was most commonly used in all age groups and there was a non-significant trend towards a higher proportion of IgA2 sequences with age (p=0.0960, Kruskal-Wallis) (**Figure 6**).

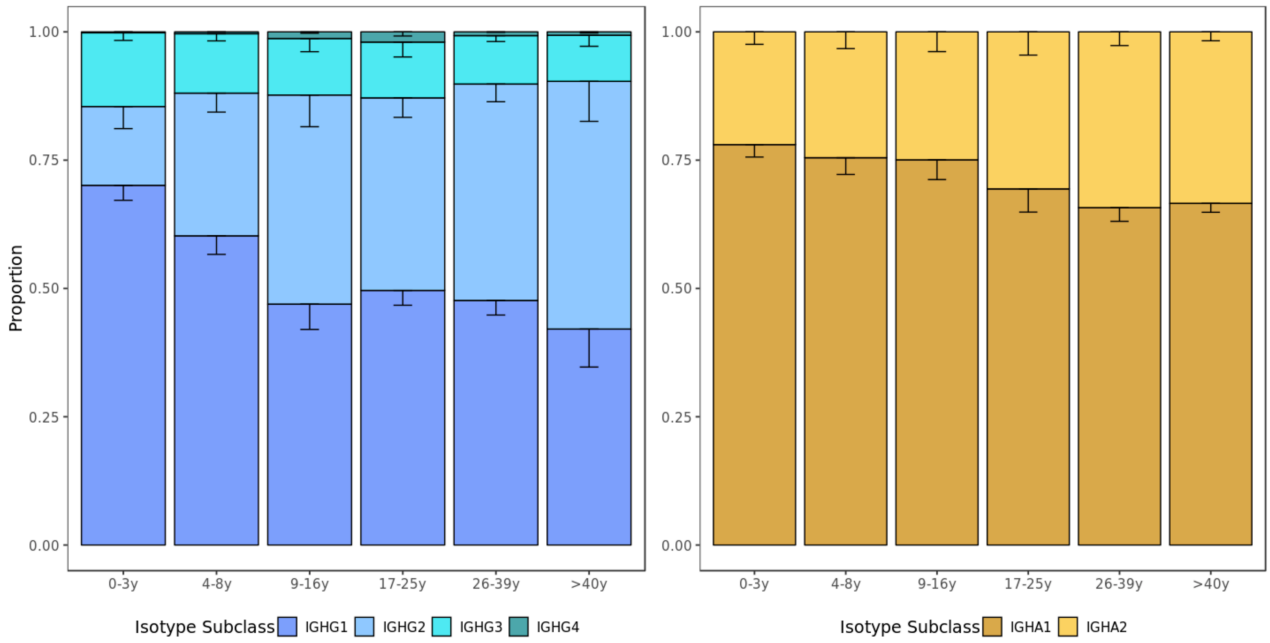

Figure 6: Usage of IgG and IgA subclasses by age group. The IgG and IgA isotype subclass usage changes with age. Error bars represent standard error of the mean.

Repertoires from older individuals contain more self-tolerant sequences

Self-reactive antibodies share sequence characteristics that can be explored by Ig-seq. These include an increased usage of certain V genes, mainly VH4-34, and usage of longer CDR3 with positively charged or hydrophobic residues (40–42). We investigated how these metrics vary with age in healthy individuals. Apart from the decreasing junction length in IgG subsets (**Figure 1C**), we found that age has no impact on charge or hydrophobicity of BCR repertoires (**Supplementary figure 8**). VH4-34 usage was also unrelated to age whereas a more detailed SHM analysis including self-reactive motifs of VH4-34 sequences revealed an age-specific pattern. The VH4-34 germline contains an Ala-Val-Tyr (AVY) hydrophobic patch in FWR1 that is not present in other V segments and is thought to contribute to the self-reactive property of this gene (43, 44). Another feature of the VH4-34 germline associated with autoimmunity is the presence of an Asn-X-Ser N-glycosylation sequon (NHS) in CDR2 that modulates antibody avidity (45). Previous research has shown that mutating one or both of these motifs drives specificity of these sequences away from self, thereby contributing to peripheral tolerance. Lower frequencies of both unmutated AVY and NHS were present in healthy elderly individuals while there was a relative accumulation of single and double-mutated motifs in VH4-34 with age (**Figure 7**). This pattern was observed across all antigen-experienced subsets but was only statistically significant for IgA and IgG antibody (p=0.0110 and p=0.0036 respectively; p=0.1800 for IgM/IgD memory; Kruskal-Wallis test).

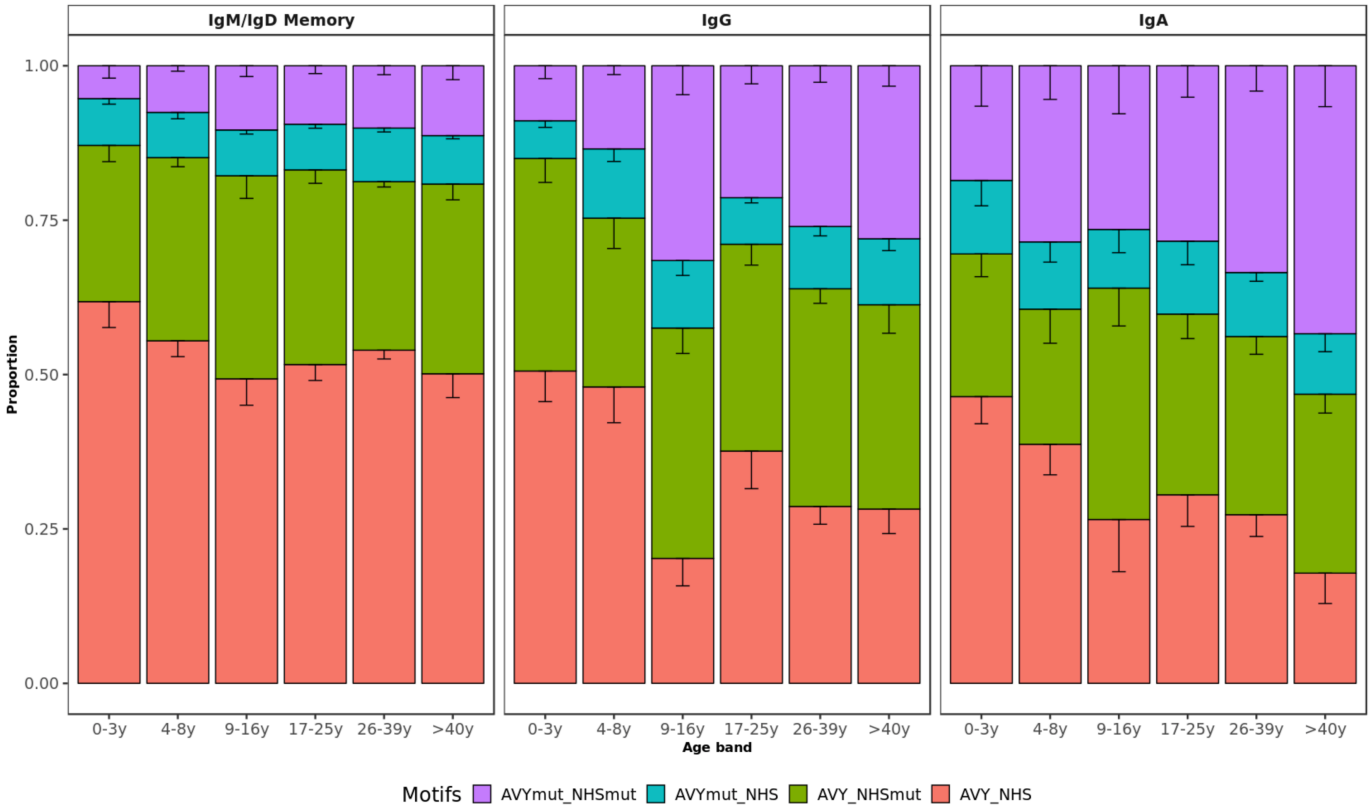

Figure 7: VH4-34 motifs by age group. Bar plots represent the proportion of sequences with mutated AVY and/or NHS motifs in IgD/IgM, IgG and IgA. Error bars indicate standard error of the mean. Proportion of sequences with both unmutated motifs decreases with age.

Combining age-related repertoire features distinguishes between children and adults

Principal component analysis (PCA) based on the age-driven variables including mutation, R/S ratio, junction length, gene usage and proportion of sequences structurally divergent from germline clearly showed distinct grouping of children younger than 9 years old and individuals older than 10 years old in antigen experienced repertoires. This distinction was most clearly observed in the class-switched IgG and IgA repertoires. In IgD/IgM mutated sequences, children less than three years old were separate from other individuals whereas the repertoire characteristics in older age categories overlapped.

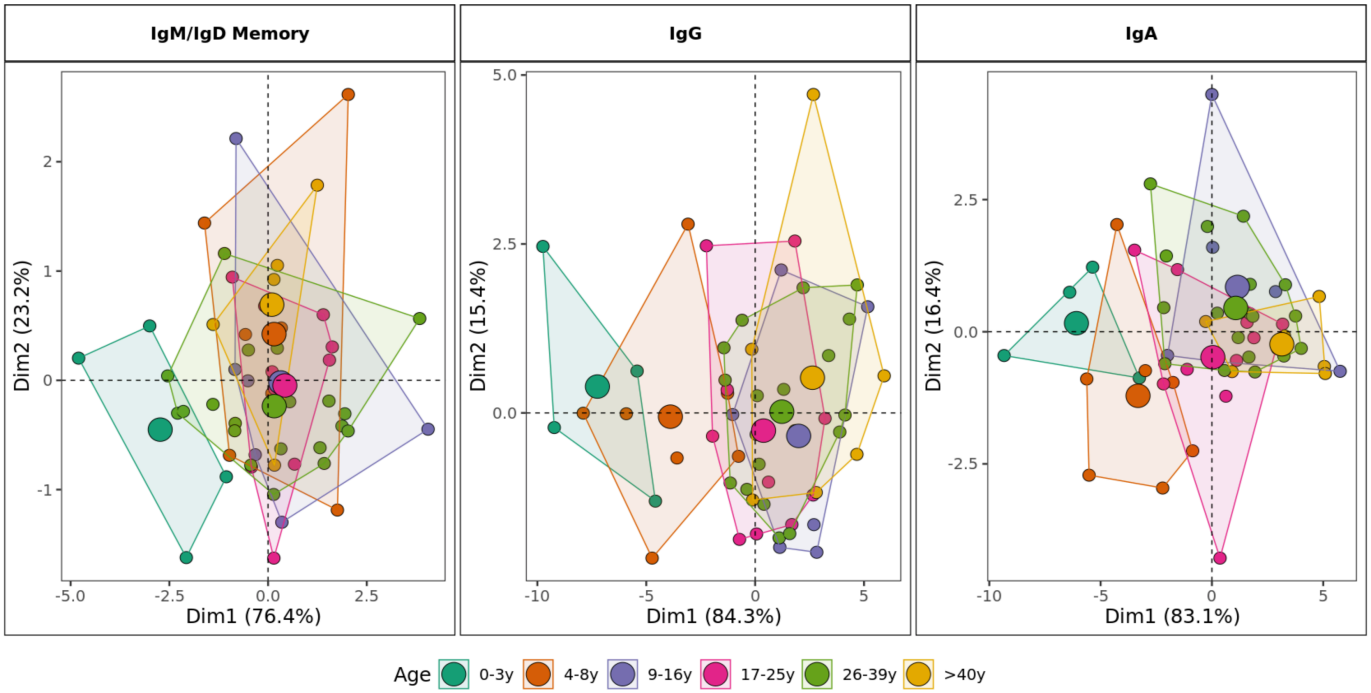

Figure 8 Stratification of BCR repertoires by age group. Principal component analysis by age category including mutation rate, R/S ratio, V1 gene family usage, J6 gene usage, junction length and proportion of sequences structurally divergent from germline as variables. For class-switched IgG and IgA, the proportion of IgG2 and IgA1 are included respectively. Areas are the convex hulls of the age group and the largest point of one color represents the center of that hull.

Discussion

In this study, we found an extensive maturation of B-cell responses in the first 10 years of life consistent with what would be expected with cumulative antigen exposure and a generally more developed and stable B-cell compartment in older individuals. Further antibody repertoire alterations continue to be made thereafter, although at a lower rate. The results presented here constitute the most in-depth evaluation of the BCR repertoire with age. This study also provides a detailed reference data set of isotype and subclass-specific BCR repertoires of healthy individuals across a relevant age range and stresses the importance of using well-selected, age-appropriate controls in future studies.

Previous studies have suggested that immunoglobulin gene usage is strongly genetically determined as it was conserved between monozygotic twins and across multiple time points within a given individual (7, 33). We found age-dependent alterations in both V family and J gene usage in antigen-experienced repertoires suggesting either polyclonal negative selection of V1- and J6-containing B cells or positive selection of non-V1/J6-bearing B cells during maturation of the adaptive immune system. However, here we also saw that V family gene usage changed in naïve repertoires that are supposedly unaffected by antigen exposure and not subject to antigen-driven selection pressure, indicating preferential development and/or survival of V1-bearing B cells in young children. Although the potential benefit and mechanism behind these age-related V family gene alterations remain unclear, these findings suggest that immunoglobulin gene usage in developing B cells is less conserved than previously thought.

In line with earlier findings (11, 46, 47), we observed extensive maturation of antigen-experienced repertoires characterized by accumulation of somatically hypermutated B-cell antibody with evidence of strong positive selection in older individuals. The observed decrease in selection pressure in some class-switched subsets indicates that young individuals show accelerated dynamics to achieve highly selected sequences compared with older individuals. Of note, detailed analysis allowed to investigate characteristics of mutated IgM/D antibody separately, which were observed at a higher frequency and with a greater number of mutations in older individuals. These findings indicate that the pool of circulating peripheral blood naïve B cells is continuously diminishing with age, possibly contributing to a decreasing capacity to effectively respond to novel antigens in older individuals (48). We also observed a substantially higher proportion of unmutated IgA/G antibody in young children compared with adults (49), a finding that has not yet been recognized and is of unknown significance. However, these results are in line with previous *in vitro* studies (50) demonstrating that class-switch recombination and somatic hypermutation can occur independently and suggest class-switching to be an important element of B-cell responses in young children.

Along with other characteristics indicative of antigen-driven maturation we found that the proportion of sequences with structures differing from germline increased with age, which was most pronounced for IgG1 and IgA1 subsets. To date, there is limited information on predicted antibody structures derived from high-throughput adaptive immune receptor repertoire sequencing data (51, 52). In line with measures of antigen-driven selection, there was a positive linear relationship between number of mutations and structural alterations of antigen-experienced sequences indicating that alteration of the three-dimensional structure is important to achieve high specificity and affinity of the antibody. By annotating individual sequences with PDB codes, we were able to investigate commonalities of CDR3 structures between individuals. In particular, in contrast to sharing on the sequence level, the majority of PDB clusters were public while only a very small percentage of PDB clusters were private to the individual. Although this comparison is influenced by the much smaller number of potential PDB clusters, the use of common PDB clusters indicates that a large number of different sequences can underlie similar antibody structures. Future work, such as the investigation of PDB usage in patients with immune disorders, will help determine how antibody structures can be used to assess global immune responses.

We found an increase in the usage of IgA2/IgG2 antibody with age, similar to what has been seen in a recent study on the isotype subclasses surface expression of peripheral blood B cells (53). While human IgG subclasses have been extensively studied (54), there is limited information on the functional difference between the two IgA subclasses, whose structures mainly differ in the length of the hinge region (55). IgG2 has been implicated in the immune responses to capsular polysaccharides of bacteria such as *S. pneumoniae* that are commonly colonizing the oropharynx of young children and thereby induce polysaccharide-specific serum antibody (56). Our findings also match the sequential model proposed for CSR: with age, and after multiple encounter with the same antigen, class-switched memory B cells re-enter the germinal center to undergo a second round of CSR and switch towards more downstream constant region genes (57).

The majority of early immature human B cells display self-reactivity and although most of these are removed during B-cell development, a substantial proportion of mature B cells may still be directed against autoantigens (40). Antibodies encoded by germline VH4-34 are intrinsically self-reactive antibodies mediated by a hydrophobic patch and a glycosylation sequon (43, 45). Unmutated VH4-34 antibody are more common in naïve than antigen-experienced repertoires as receptor editing of these antibodies drives specificity away from self (44, 58). In contrast to adults, we found that a substantial proportion of VH4-34 IgG and IgA antibody from children are unmutated, with frequencies gradually decreasing with age. Previous work has shown that germline VH4-34-expressing IgG B cells recognized antigens from commensal gut bacterial (58) and hence, the higher frequency of these cells in children may be related to ongoing immune responses against gut pathogens in this age group.

This study used Ig-seq technology coupled with bioinformatic methods to study in detail the BCR repertoires of healthy individuals and investigate the effect of age on repertoire characteristics. We chose a cross-sectional study design and – although unlikely – can therefore not exclude that longitudinal assessment of maturation on an individual basis may differ from the presented findings. For practical reasons, the number of input cells was variable between study participants, which resulted in variable sequence numbers per sample. For analysis where sequence number variability was considered to be of major relevance, such as constructing lineage trees, subsampling to an equal number of sequences per individual was performed.

We were able to map in detail the characteristics, magnitude and speed of age-dependent maturation of BCR repertoires. Combining age-related variables using a PCA allowed clear separation of individuals younger than 10 years from older study participants, which was most pronounced in IgG repertoires. Our analysis now allows comparisons to be made in the BCR repertoires of healthy individuals to patients with altered immune states such as primary or secondary immunodeficiency (4) or infectious disease (59, 60). By elucidating patterns that are associated with cumulative antigen exposure and an evolving immune system, this research offers important insight into adaptive immune system responses in humans. The mechanisms behind the development of clinically relevant autoimmunity is still poorly understood and the findings in this study show a substantial intrinsic capacity to produce self-reactive B cells, which may be essential to achieve the diversity needed for the defense against commensal pathogens in early life.

In summary, by studying the maturation of the healthy BCR repertoire with age, we found characteristics indicative of a maturing B-cell system consisting of alterations in immunoglobulin gene usage, increased levels of SHM associated with strong positive selection, and canonical class usage that differed considerably from germline structures. Repertoires from older individuals more frequently contained antibody using more downstream constant region genes that are involved in the immune response to polysaccharide antigens. With accumulating mutations, germline-encoded self-reactive antibody were seen less with advancing age indicating a possible beneficial role of self-reactive B-cells in the developing immune system. This study provides a reference data set of isotype subclass-specific BCR repertoires and stresses the importance of using well-selected, age-appropriate controls in future studies.

References

1. Reich, N. C. 2008. Janeway's Immunobiology . Seventh Edition. By *Kenneth Murphy, Paul Travers,* and *, Mark Walport; contributions by, Michael Ehrenstein, Claudia Mauri, Allan Mowat,* and *, Andrey Shaw.* Garland Science . *New York: Taylor &amp*, 7th ed. (K. Murphy, P. Travers, and M. Walport, eds). Garland Science, New York and London.

2. Rawlings, D. J., G. Metzler, M. Wray-Dutra, and S. W. Jackson. 2017. Altered B cell signalling in autoimmunity. *Nat. Rev. Immunol.* 17: 421–436.

3. Hoffman, W., F. G. Lakkis, and G. Chalasani. 2016. B Cells, Antibodies, and More. *Clin. J. Am. Soc. Nephrol.* 11: 137–54.

4. Ghraichy, M., J. D. Galson, D. F. Kelly, and J. Trück. 2018. B-cell receptor repertoire sequencing in patients with primary immunodeficiency: a review. *Immunology* 153: 145–160.

5. Bashford-Rogers, R. J. M., K. G. C. Smith, and D. C. Thomas. 2018. Antibody repertoire analysis in polygenic autoimmune diseases. *Immunology* 155: 3–17.

6. Jiang, N., J. He, J. A. Weinstein, L. Penland, S. Sasaki, X. S. He, C. L. Dekker, N. Y. Zheng, M. Huang, M. Sullivan, P. C. Wilson, H. B. Greenberg, M. M. Davis, D. S. Fisher, and S. R. Quake. 2013. Lineage structure of the human antibody repertoire in response to influenza vaccination. *Sci. Transl. Med.* 5: 171ra19.

7. Galson, J. D., J. Trück, E. A. Clutterbuck, A. Fowler, V. Cerundolo, A. J. Pollard, G. Lunter, and D. F. Kelly. 2016. B-cell repertoire dynamics after sequential hepatitis B vaccination and evidence for cross-reactive B-cell activation. *Genome Med.* 8: 68.

8. Galson, J. D., J. Trück, A. Fowler, M. Münz, V. Cerundolo, A. J. Pollard, G. Lunter, and D. F. Kelly. 2015. In-depth assessment of within-individual and inter-individual variation in the B cell receptor repertoire. *Front. Immunol.* 6: 1–13.

9. Galson, J. D., E. A. Clutterbuck, J. Trück, M. N. Ramasamy, M. Münz, A. Fowler, V. Cerundolo, A. J. Pollard, G. Lunter, and D. F. Kelly. 2015. BCR repertoire sequencing: Different patterns of B-cell activation after two Meningococcal vaccines. *Immunol. Cell Biol.* 93: 885–895.

10. Kovaltsuk, A., J. Leem, S. Kelm, J. Snowden, C. M. Deane, and K. Krawczyk. 2018. Observed Antibody Space: A Resource for Data Mining Next-Generation Sequencing of Antibody Repertoires. *J. Immunol.* 201: 2502–2509.

11. IJspeert, H., P. A. van Schouwenburg, D. van Zessen, I. Pico-Knijnenburg, G. J. Driessen, A. P. Stubbs, and M. van der Burg. 2016. Evaluation of the antigen-experienced B-cell receptor repertoire in healthy children and adults. *Front. Immunol.* 7: 410.

12. Comans-Bitter, W. M., R. De Groot, R. Van den Beemd, H. J. Neijens, W. C. J. Hop, K. Groeneveld, H. Hooijkaas, and J. J. M. Van Dongen. 1997. Immunophenotyping of blood lymphocytes in childhood: Reference values for lymphocyte subpopulations. *J. Pediatr.* 130: 388–393.

13. Vander Heiden, J. A., G. Yaari, M. Uduman, J. N. H. Stern, K. C. O'connor, D. A. Hafler, F. Vigneault, and S. H. Kleinstein. 2014. PRESTO: A toolkit for processing high-throughput sequencing raw reads of lymphocyte receptor repertoires. *Bioinformatics* 30: 1930–1932.

14. Gupta, N. T., J. A. Vander Heiden, M. Uduman, D. Gadala-Maria, G. Yaari, and S. H. Kleinstein. 2015. Change-O: A toolkit for analyzing large-scale B cell immunoglobulin repertoire sequencing data. *Bioinformatics* 31: 3356–3358.

15. Ye, J., N. Ma, T. L. Madden, and J. M. Ostell. 2013. IgBLAST: an immunoglobulin variable domain sequence analysis tool. *Nucleic Acids Res.* 41: W34–W40.

16. Lunter, G., and M. Goodson. 2011. Stampy: A statistical algorithm for sensitive and fast mapping of Illumina sequence reads. *Genome Res.* 21: 936–939.

17. Stern, J. N. H., G. Yaari, J. A. Vander Heiden, G. Church, W. F. Donahue, R. Q. Hintzen, A. J. Huttner, J. D. Laman, R. M. Nagra, A. Nylander, D. Pitt, S. Ramanan, B. A. Siddiqui, F. Vigneault, S. H. Kleinstein, D. A. Hafler, and K. C. O'Connor. 2014. B cells populating the multiple sclerosis brain mature in the draining cervical lymph nodes. *Sci. Transl. Med.* 6: 248ra107-248ra107.

18. Yaari, G., M. Uduman, and S. H. Kleinstein. 2012. Quantifying selection in high-throughput Immunoglobulin sequencing data sets. *Nucleic Acids Res.* 40: 1–10.

19. Kovaltsuk, A., M. I. J. Raybould, W. K. Wong, C. Marks, S. Kelm, J. Snowden, J. Trück, and C. M. Deane. 2019. Structural Diversity of B-Cell Receptor Repertoires along the B-cell Differentiation Axis in Humans and Mice. *bioRxiv* 762880.

20. Lefranc, M. P., C. Pommié, M. Ruiz, V. Giudicelli, E. Foulquier, L. Truong, V. Thouvenin-Contet, and G. Lefranc. 2003. IMGT unique numbering for immunoglobulin and T cell receptor variable domains and Ig superfamily V-like

domains. *Dev. Comp. Immunol.* 27: 55–77.

21. Dunbar, J., and C. M. Deane. 2015. ANARCI: Antigen receptor numbering and receptor classification. *Bioinformatics* 32: 298–300.

22. Kovaltsuk, A., K. Krawczyk, S. Kelm, J. Snowden, and C. M. Deane. 2018. Filtering Next-Generation Sequencing of the Ig Gene Repertoire Data Using Antibody Structural Information. *J. Immunol.* 201: 3694–3704.

23. Wong, W. K., G. Georges, F. Ros, S. Kelm, A. P. Lewis, B. Taddese, J. Leem, and C. M. Deane. 2019. SCALOP: Sequence-based antibody canonical loop structure annotation. *Bioinformatics* 35: 1774–1776.

24. Choi, Y., and C. M. Deane. 2010. FREAD revisited: Accurate loop structure prediction using a database search algorithm. *Proteins Struct. Funct. Bioinforma.* 78: 1431–1440.

25. Berman, H., K. Henrick, H. Nakamura, and J. L. Markley. 2007. The worldwide Protein Data Bank (wwPDB): Ensuring a single, uniform archive of PDB data. *Nucleic Acids Res.* 35.

26. R Core Team. 2019. R: A language and environment for statistical computing. .

27. Wickham, H. 2016. *ggplot2: Elegant Graphics for Data Analysis*,. Springer-Verlag New York.

28. Kassambara, A. 2019. ggpubr: “ggplot2” Based Publication Ready Plots. *R Packag. version 0.1.8.* .

29. Gu, Z., R. Eils, and M. Schlesner. 2016. Complex heatmaps reveal patterns and correlations in multidimensional genomic data. *Bioinformatics* 32: 2847–2849.

30. Kassambara, A., and F. Mundt. 2017. Package “factoextra” for R: Extract and Visualize the Results of Multivariate Data Analyses. *R Packag. version* .

31. Luo, S., J. A. Yu, and Y. S. Song. 2016. Estimating Copy Number and Allelic Variation at the Immunoglobulin Heavy Chain Locus Using Short Reads. *PLoS Comput. Biol.* 12: e1005117.

32. Rubelt, F., C. E. Busse, S. A. C. Bukhari, J. P. Bürckert, E. Mariotti-Ferrandiz, L. G. Cowell, C. T. Watson, N. Marthandan, W. J. Faison, U. Hershberg, U. Laserson, B. D. Corrie, M. M. Davis, B. Peters, M. P. Lefranc, J. K. Scott, F. Breden, E. T. Luning Prak, and S. H. Kleinstein. 2017. Adaptive Immune Receptor Repertoire Community recommendations for sharing immune-repertoire sequencing data. *Nat. Immunol.* 18: 1274–1278.

33. Glanville, J., T. C. Kuo, H.-C. von Budingen, L. Guey, J. Berka, P. D. Sundar, G. Huerta, G. R. Mehta, J. R. Oksenberg, S. L. Hauser, D. R. Cox, A. Rajpal, and J. Pons. 2011. Naive antibody gene-segment frequencies are heritable and unaltered by chronic lymphocyte ablation. *Proc. Natl. Acad. Sci.* 108: 20066–20071.

34. Briney, B., A. Inderbitzin, C. Joyce, and D. R. Burton. 2019. Commonality despite exceptional diversity in the baseline human antibody repertoire. *Nature* 566: 393–397.

35. Donisi, P. M., N. Di Lorenzo, M. Riccardi, A. Paparella, C. Sarpellon, S. Zupo, G. Bertoldero, C. Minotto, and V. Stracca-Pansa. 2006. Pattern and distribution of immunoglobulin VH gene usage in a cohort of B-CLL patients from a northeastern region of Italy. *Diagnostic Mol. Pathol.* 15: 206–215.

36. Widhopf, G. F., L. Z. Rassenti, T. L. Toy, J. G. Gribben, W. G. Wierda, and T. J. Kipps. 2004. Chronic lymphocytic leukemia B cells of more than 1% of patients express virtually identical immunoglobulins. *Blood* 104: 2499–2504.

37. North, B., A. Lehmann, and R. L. Dunbrack. 2011. A new clustering of antibody CDR loop conformations. *J. Mol. Biol.* 406: 228–256.

38. Chothia, C., and A. M. Lesk. 1987. Canonical structures for the hypervariable regions of immunoglobulins. *J. Mol. Biol.* 196: 901–917.

39. Tsioris, K., N. T. Gupta, A. O. Ogunniyi, R. M. Zimnisky, F. Qian, Y. Yao, X. Wang, J. N. H. Stern, R. Chari, A. W. Briggs, C. R. Clouser, F. Vigneault, G. M. Church, M. N. Garcia, K. O. Murray, R. R. Montgomery, S. H. Kleinstein, and J. C. Love. 2015. Neutralizing antibodies against West Nile virus identified directly from human B cells by single-cell analysis and next generation sequencing. *Integr. Biol.* 7: 1587–1597.

40. Wardemann, H., S. Yurasov, A. Schaefer, J. W. Young, E. Meffre, and M. C. Nussenzweig. 2003. Predominant autoantibody production by early human B cell precursors. *Science (80-.).* 301: 1374–1377.

41. Larimore, K., M. W. McCormick, H. S. Robins, and P. D. Greenberg. 2012. Shaping of Human Germline IgH Repertoires Revealed by Deep Sequencing. *J. Immunol.* 189: 3221–3230.

42. Pugh-Bernard, A. E., G. J. Silverman, A. J. Cappione, M. E. Villano, D. H. Ryan, R. A. Insel, and I. Sanz. 2001. Regulation of inherently autoreactive VH4-34 B cells in the maintenance of human B cell tolerance. *J. Clin. Invest.* 108: 1061–1070.

43. Potter, K. N., P. Hobby, S. Klijn, F. K. Stevenson, and B. J. Sutton. 2002. Evidence for involvement of a hydrophobic patch in framework region 1 of human V4-34-encoded Igs in recognition of the red blood cell I antigen.

J. Immunol. 169: 3777–3782.

44. Reed, J. H., J. Jackson, D. Christ, and C. C. Goodnow. 2016. Clonal redemption of autoantibodies by somatic hypermutation away from self-reactivity during human immunization. *J. Exp. Med.* 213: 1255–1265.

45. Sabouri, Z., P. Schofield, K. Horikawa, E. Spierings, D. Kipling, K. L. Randall, D. Langley, B. Roome, R. Vazquez-Lombardi, R. Rouet, J. Hermes, T. D. Chan, R. Brink, D. K. Dunn-Walters, D. Christ, and C. C. Goodnow. 2014. Redemption of autoantibodies on anergic B cells by variable-region glycosylation and mutation away from self-reactivity. *Proc. Natl. Acad. Sci.* 111: E2567–E2575.

46. Tabibian-Keissar, H., L. Hazanov, G. Schiby, N. Rosenthal, A. Rakovsky, M. Michaeli, G. L. Shahaf, Y. Pickman, K. Rosenblatt, D. Melamed, D. Dunn-Walters, R. Mehr, and I. Barshack. 2016. Aging affects B-cell antigen receptor repertoire diversity in primary and secondary lymphoid tissues. *Eur. J. Immunol.* 46: 480–492.

47. Schatorjé, E. J. H., G. J. Driessen, R. W. N. M. van Hout, M. van der Burg, and E. de Vries. 2014. Levels of somatic hypermutations in B cell receptors increase during childhood. *Clin. Exp. Immunol.* 178: 394–398.

48. Siegrist, C. A., and R. Aspinall. 2009. B-cell responses to vaccination at the extremes of age. *Nat. Rev. Immunol.* 9: 185–194.

49. Fecteau, J. F., G. Cote, and S. Neron. 2006. A New Memory CD27-IgG+ B Cell Population in Peripheral Blood Expressing VH Genes with Low Frequency of Somatic Mutation. *J. Immunol.* 177: 3728–3736.

50. Nagumo, H., K. Agematsu, N. Kobayashi, K. Shinozaki, S. Hokibara, H. Nagase, M. Takamoto, K. Yasui, K. Sugane, and A. Komiyama. 2002. The different process of class switching and somatic hypermutation; a novel analysis by CD27-naive B cells. *Blood* 99: 567–575.

51. Kovaltsuk, A., K. Krawczyk, J. D. Galson, D. F. Kelly, C. M. Deane, and J. Trück. 2017. How B-cell receptor repertoire sequencing can be enriched with structural antibody data. *Front. Immunol.* 8: 1753.

52. Krawczyk, K., S. Kelm, A. Kovaltsuk, J. D. Galson, D. Kelly, J. Trück, C. Regep, J. Leem, W. K. Wong, J. Nowak, J. Snowden, M. Wright, L. Starkie, A. Scott-Tucker, J. Shi, and C. M. Deane. 2018. Structurally mapping antibody repertoires. *Front. Immunol.* 9.

53. Blanco, E., M. Pérez-Andrés, S. Arriba-Méndez, T. Contreras-Sanfeliciano, I. Criado, O. Pelak, A. Serra-Caetano, A. Romero, N. Puig, A. Remesal, J. Torres Canizales, E. López-Granados, T. Kalina, A. E. Sousa, M. van Zelm, M. van der Burg, J. J. M. van Dongen, and A. Orfao. 2018. Age-associated distribution of normal B-cell and plasma cell subsets in peripheral blood. *J. Allergy Clin. Immunol.* 141: 2208-2219.e16.

54. Vidarsson, G., G. Dekkers, and T. Rispens. 2014. IgG subclasses and allotypes: From structure to effector functions. *Front. Immunol.* 5: 520.

55. Woof, J. M., and M. A. Kerr. 2004. IgA function - Variations on a theme. *Immunology* 113: 175–177.

56. Turner, P., C. Turner, N. Green, L. Ashton, E. Lwe, A. Jankhot, N. P. Day, N. J. White, F. Nosten, and D. Goldblatt. 2013. Serum antibody responses to pneumococcal colonization in the first 2 years of life: Results from an SE Asian longitudinal cohort study. *Clin. Microbiol. Infect.* 19: 1–8.

57. Xiong, H., J. Dolpady, M. Wabl, M. A. Curotto de Lafaille, and J. J. Lafaille. 2012. Sequential class switching is required for the generation of high affinity IgE antibodies. *J. Exp. Med.* 209: 353–364.

58. Schickel, J.-N., S. Glauzy, Y.-S. Ng, N. Chamberlain, C. Massad, I. Isnardi, N. Katz, G. Uzel, S. M. Holland, C. Picard, A. Puel, J.-L. Casanova, and E. Meffre. 2017. Self-reactive VH4-34–expressing IgG B cells recognize commensal bacteria. *J. Exp. Med.* 214: 1991–2003.

59. Hou, D., C. Chen, E. J. Seely, S. Chen, and Y. Song. 2016. High-throughput sequencing-based immune repertoire study during infectious disease. *Front. Immunol.* 7: 336.

60. Burkholder, W. F., E. W. Newell, M. Poidinger, S. Chen, and K. Fink. 2017. Deep Sequencing in Infectious Diseases: Immune and Pathogen Repertoires for the Improvement of Patient Outcomes. *Front. Immunol.* 8: 593.

Supplementary information

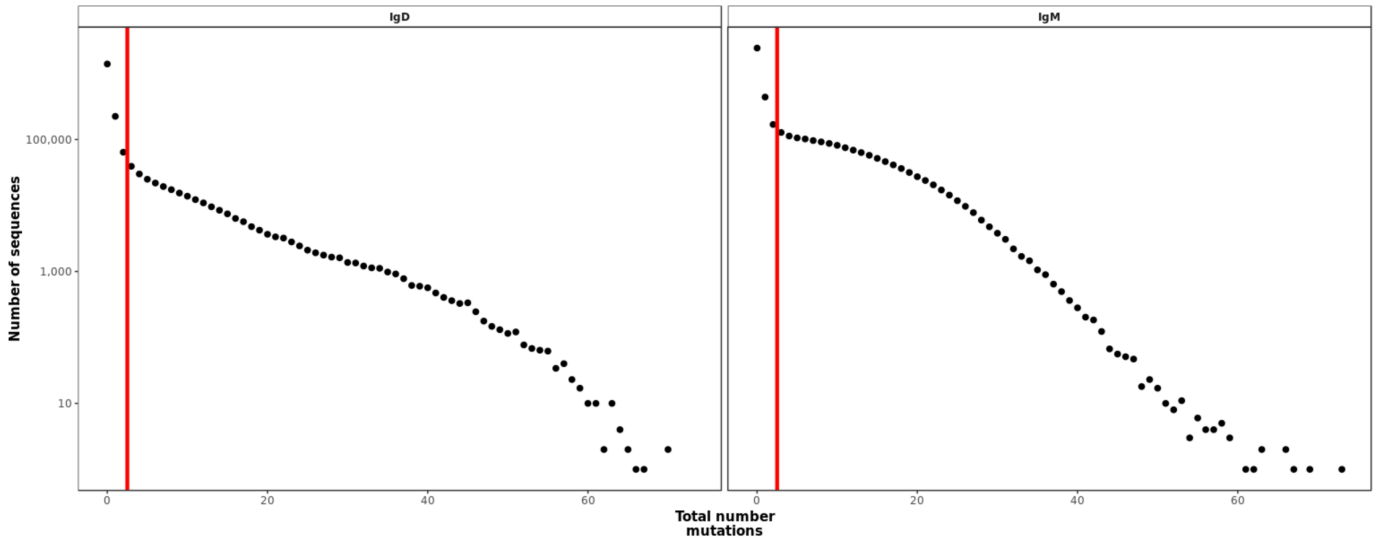

Supplementary figure 1 Distribution of somatic hypermutation in all IgD and IgM transcripts. The vertical line indicates the threshold chosen (mutation n between 2 and 3) to separate naïve and memory repertoires for IgM and IgD sequences.

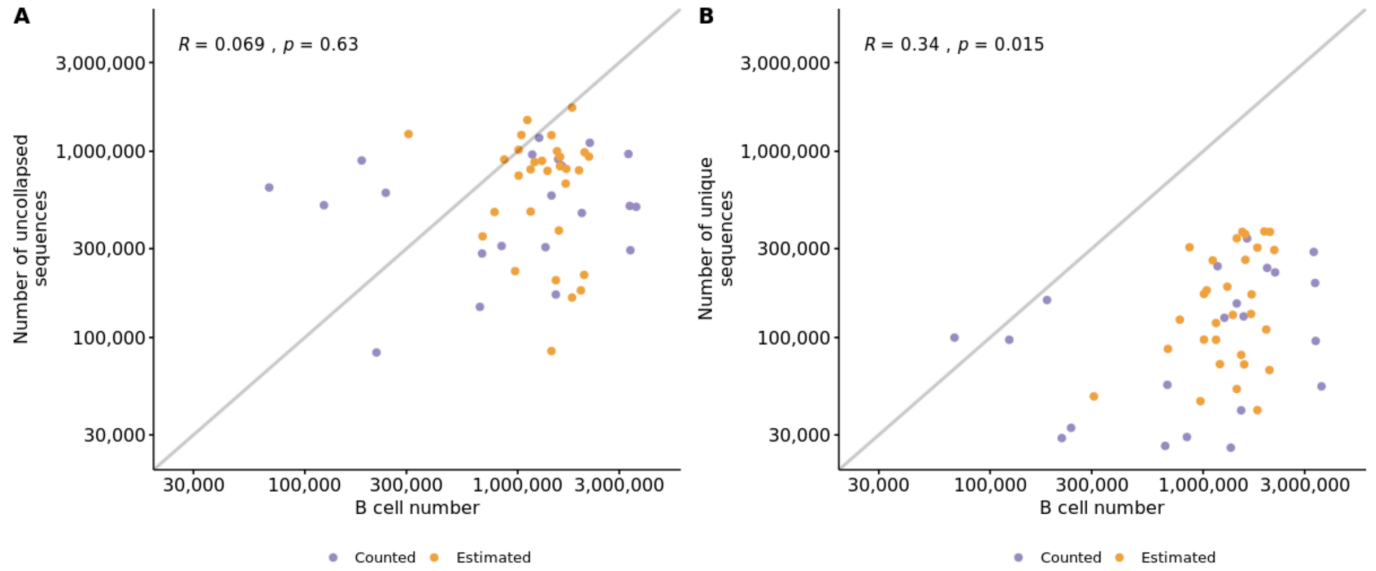

Supplementary figure 2: Correlation between cell number in a sample, and the number of sequences for that sample *A* before and *B* after collapsing (Pearson correlation coefficient). The B-cell number was either based on actual counts or estimated using PBMC counts and the median percentage of age-dependent reference values.

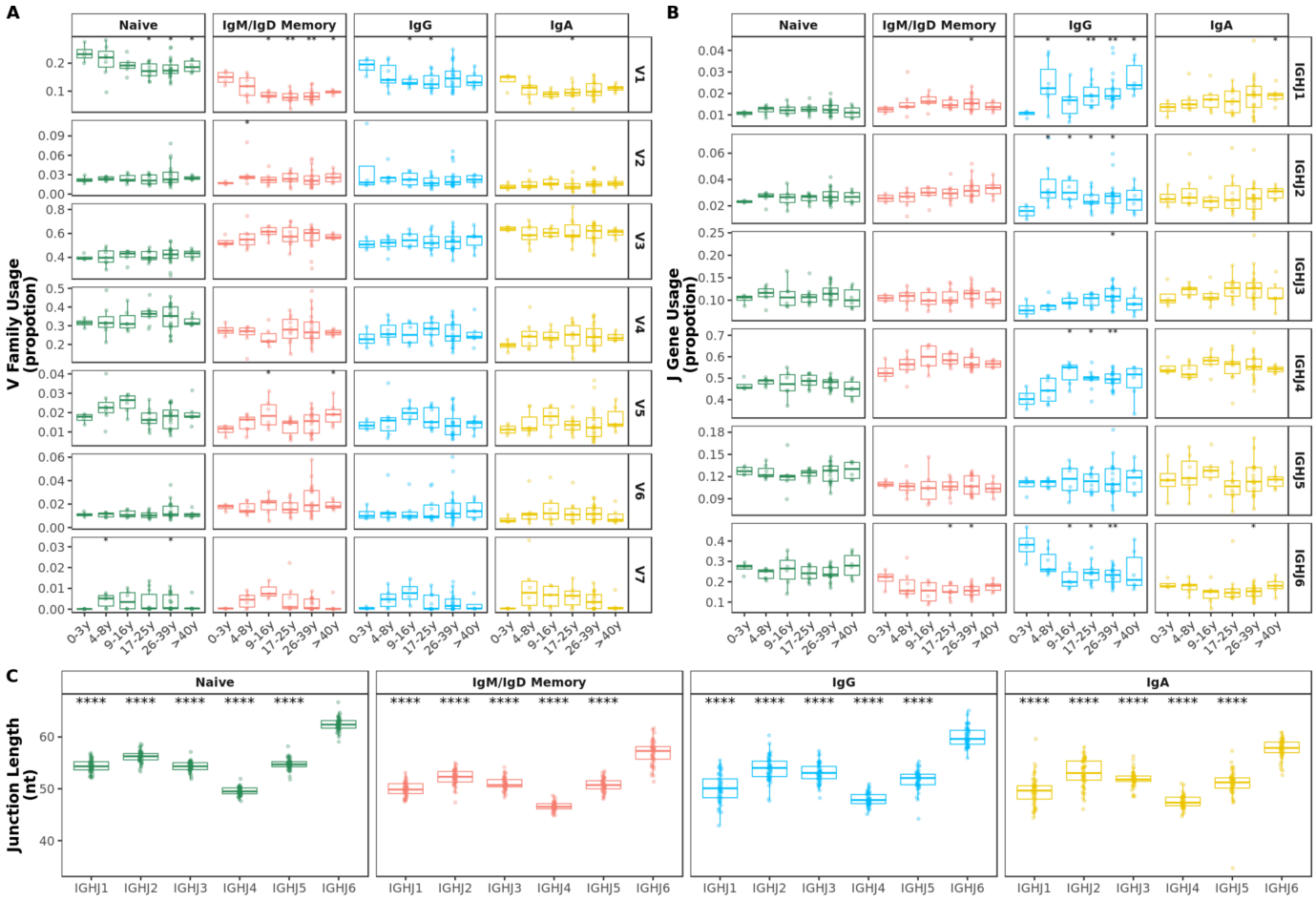

Supplementary figure 3 *A* V family and *B* J gene usage by age band. Comparison of each age group to the 0-3y group was performed using the Wilcoxon test. *C* IGHJ6 transcripts show significantly longer junctions. Comparison of each gene to IGHJ6 was performed using the Wilcoxon test. *p<0.05, **p<0.01, ***p<0.001, ****p<0.0001

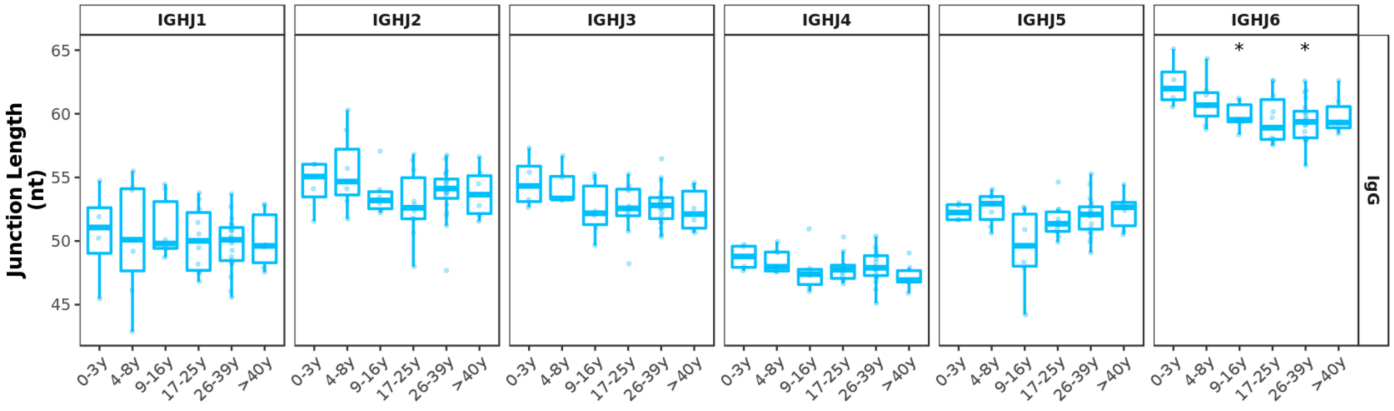

Supplementary Figure 4: Junction length decrease in IgG transcripts is still apparent within J gene and is only significant in transcripts with IGHJ6. Comparison of each age group to the 0-3y group was performed using the Wilcoxon test. *p<0.05

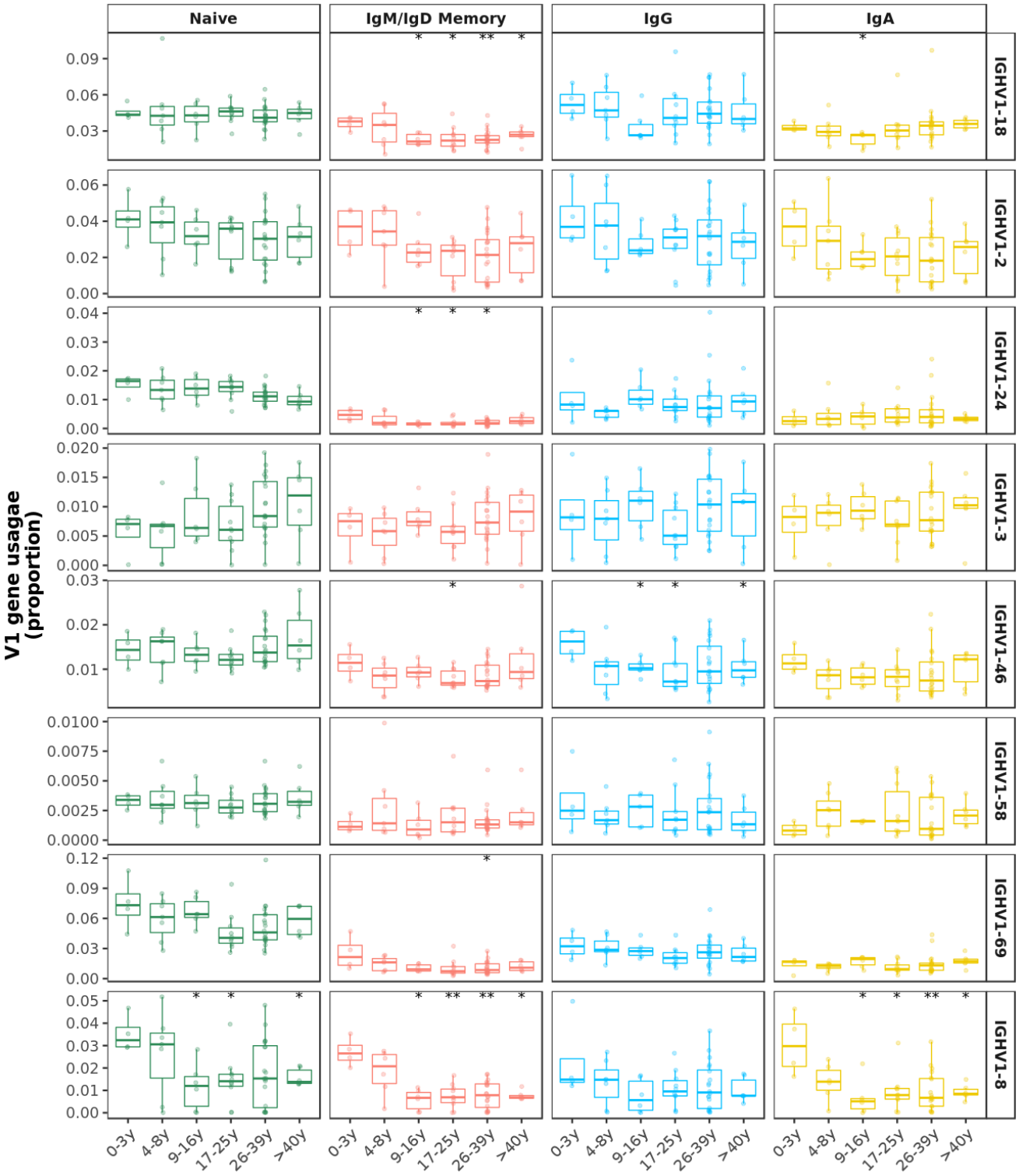

Supplementary figure 5 Proportion of the top 8 V1 family genes by age band. The decrease seen in V1 family usage is a result of a decrease in multiple individual genes. Comparison of each age group to the 0-3y group was performed using the Wilcoxon test. *p<0.05, **p<0.01

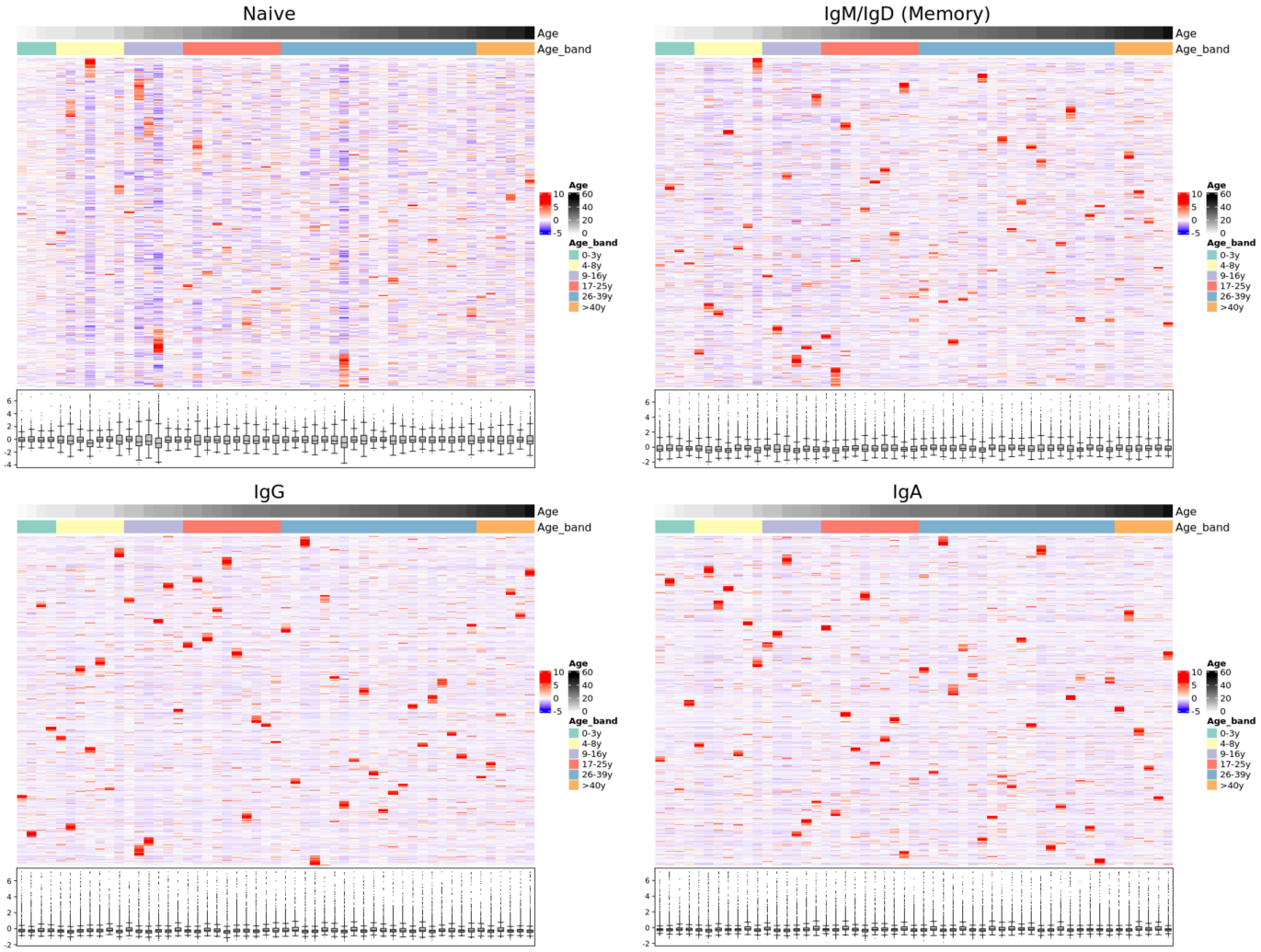

Supplementary Figure 6 The structural composition of the naïve, IgM/IgD memory and class-switched IgG and IgA repertoires. Heatmaps are normalized by row which represents usage of one PDB cluster. Distributions of the normalized PDB cluster usage by individual is shown as a boxplot. Samples (columns) are ordered by age and PDB clusters (rows) are hierarchically clustered.

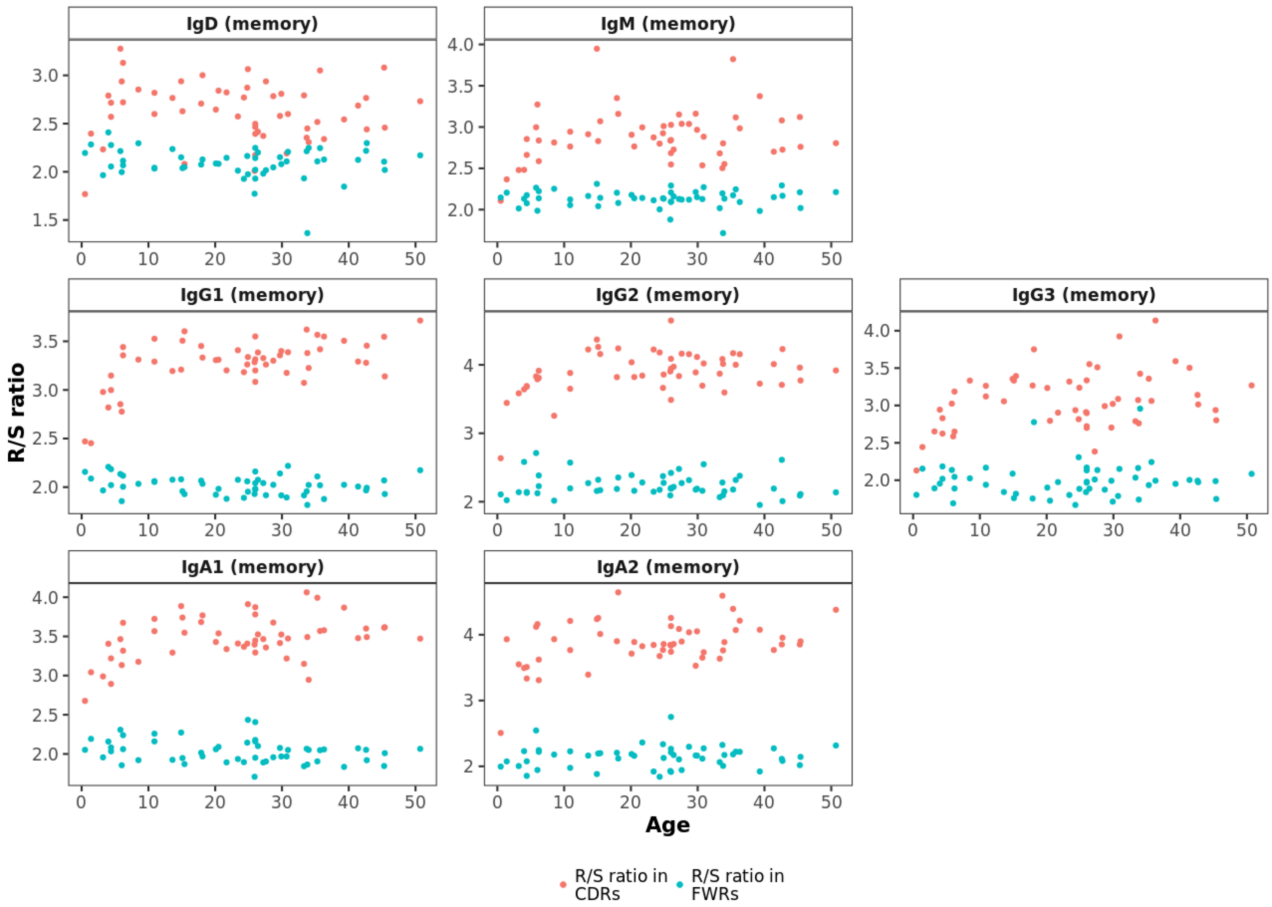

Supplementary figure 7 R/S ratio in FWRs does not correlate with age and is lower compared with CDRs.

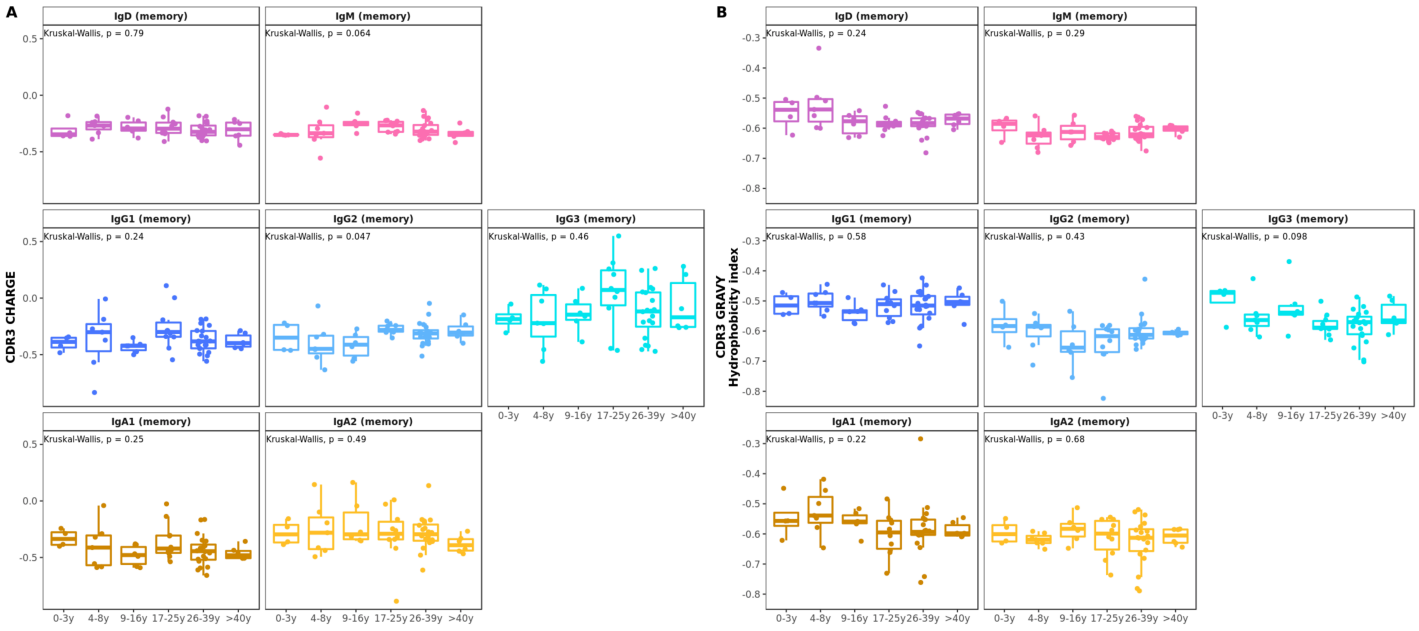

Supplementary figure 8 *A* CDR3 charge and *B* CDR3 hydrophobicity index do not correlate with age in healthy controls.

Supplementary table 1

Participant	Sex	Age (y)	Cell type	PBMC number	B cell number	B cells estimated (E) or counted (C)	RT PCR	Raw Sequences	Unique Productive Sequences	IgD (naive)	IgM (naïve)	IgD (memory)	IgM (memory)	IgG1 (memory)	IgG2 (memory)	IgG3 (memory)	IgG4 (Memory)	IgA1 (Memory)	IgA2 (memory)	IgE (memory)
HC_1	F	0.5	PBMCs	14400000	3024000	E	AEG,MD	1904663	285839	72572	159399	2240	7963	21480	4276	4875	38	9509	3429	58
HC_2	F	1.4	PBMCs	6900000	1932000	E	AEG,MD	2326250	239052	62659	132670	5230	11630	16237	1263	3647	18	4585	1111	2
HC_3	M	3.2	PBMCs	9900000	2376000	E	AEG,MD	1622639	221134	52374	115799	3386	18607	11164	4741	1819	54	9894	3246	50
HC_4	F	3.9	PBMCs	9450000	2268000	E	AEG,MD	1571312	337616	55542	156394	14433	35134	35350	6421	7459	46	22599	4230	8
HC_5	F	4.4	PBMCs	4200000	1008000	E	AEG,MD	1975420	93299	20948	44505	2070	10982	5957	3788	1587	42	2099	1280	41
HC_6	M	4.4	PBMCs	1140000	273600	E	AEG,MD	1216544	28674	13955	9161	1689	1786	872	341	122	4	599	141	4
HC_7	F	5.8	PBMCs	11100000	1998000	E	AEG,MD	1973589	128326	35276	44614	10339	9463	13050	5047	1526	53	7791	1164	3
HC_8	M	6.0	PBMCs	12600000	2268000	E	AEG,MD	1818496	124567	7399	32174	1387	22205	37668	5395	5989	34	10097	2147	72
HC_9	M	6.2	PBMCs	6150000	1107000	E	AEG,MD	2474481	255693	84048	129241	4096	12182	5861	4610	1268	46	9844	4117	380
HC_10	F	6.2	PBMCs	10800000	1944000	E	AEG,MD	1337214	368861	29803	112882	7228	54220	42616	28527	7659	534	59361	25936	95
HC_11	M	8.5	PBMCs	10800000	1944000	E	AEG,MD	880759	40494	18417	10920	1431	3099	2283	841	725	19	2126	633	0
HC_12	F	10.9	PBMCs	12900000	2064000	E	AEG,MD	1802230	366617	65222	148236	11720	72104	20972	10050	9851	427	19081	8746	208
HC_13	F	10.9	PBMCs	7920000	1267200	E	AEG,MD	1168944	25242	6459	7505	1519	5248	1829	977	261	25	1057	275	87
HC_14	F	13.6	PBMCs	4740000	758400	E	AEG,MD	872906	26006	8819	8659	2185	4714	278	644	70	5	450	173	9
HC_15	F	14.9	PBMCs	1920000	307200	E	AEG,MD	2717449	44254	1632	3581	1259	17735	5991	3376	1053	238	5918	3464	7
HC_16	M	15.1	PBMCs	14700000	2352000	E	AEG,MD	659493	95429	40827	36587	2228	6421	1635	2474	384	67	3639	1056	111
HC_17	F	15.4	PBMCs	NA	NA	NA	AEG,MD	995764	289287	41886	118609	4719	24748	37623	27409	6542	1142	24002	2592	15
HC_18	F	17.9	PBMCs	7200000	864000	E	AEG,MD	1682823	302272	26679	68526	4680	55458	37658	10783	12027	1252	77485	7704	20
HC_19	M	18.1	PBMCs	8400000	1008000	E	AEG,MD	1011146	28798	12418	7307	1269	2209	1350	870	158	151	2248	818	0
HC_20	M	20.1	PBMCs	13200000	1584000	E	AEG,MD	1433354	356105	42060	104452	5655	64801	39036	22756	4546	67	61075	11647	10
HC_21	M	20.5	PBMCs	9600000	1152000	E	AEG,MD	945221	96859	25143	28963	6092	21561	5861	3223	381	684	3195	1695	61
HC_22	M	21.7	PBMCs	15000000	1800000	E	AEG,MD	1140675	40591	21975	8263	4543	4454	294	178	244	1	477	160	2
HC_23	F	23.4	PBMCs	9000000	1080000	E	AEG,MD	1423314	151168	68644	25308	10563	9876	7757	11844	1094	88	12146	3815	33
HC_24	F	24.3	CD19+		3600000	C	AEG,MD	1650432	53250	2584	27411	648	13631	2320	2099	628	26	2098	1803	2
HC_25	F	24.8	PBMCs	17100000	2052000	E	AEG,MD	764310	66786	12784	24047	3933	17222	2397	1562	308	0	3145	1386	2
HC_26	F	24.9	PBMCs	18000000	2160000	E	AEG,MD	1683395	288827	35736	91187	6432	63062	18078	28519	2636	2025	26499	14562	91
HC_27	M	25.9	PBMCs	12000000	1440000	E	Mix I	593323	52933	7679	27223	1394	10655	2280	2011	432	17	509	728	5
HC_28	F	26.0	PBMCs	14000000	1680000	E	Mix I	1146458	133861	20396	54984	3362	27783	10845	10135	1339	123	2477	2399	18
HC_29	F	26.0	CD19+		2000000	C	AEG,MD	1710083	235120	30835	145027	3509	38873	5427	3685	1335	17	4627	1783	2
HC_30	F	26.0	PBMCs	3300000	185000	C	AEG,MD	2347978	158947	49263	63128	7051	20867	6055	4737	1279	99	5434	1033	1
HC_31	F	26.0	PBMCs	1725000	68000	C	AEG,MD	1524836	99870	25370	29303	6741	23073	4476	3962	708	102	4847	1288	0
HC_32	F	26.4	PBMCs	14100000	1692000	E	AEG,MD	1581380	168295	56857	51011	4527	10671	12723	6925	6070	230	13898	5288	95
HC_33	F	27.2	PBMCs	13000000	1560000	E	Mix I	1217105	71742	8699	28815	1976	22157	4257	2197	1173	36	1479	953	0
HC_34	F	27.6	CD19+	11250000	240000	C	AEG,MD	941177	31596	2636	6664	1330	13308	1496	2727	208	52	2155	1020	0
HC_35	F	28.7	PBMCs	8700000	1044000	E	AEG,MD	1824932	176403	17952	66414	4320	48242	11813	8105	1447	249	11565	6271	25
HC_36	F	29.7	PBMCs	8100000	972000	E	AEG,MD	1103351	45312	8848	15726	817	10931	2324	1406	233	10	3726	1291	0
HC_37	M	29.9	PBMCs	12000000	1440000	E	AEG,MD	1909727	338646	44381	139814	7439	91713	11746	23501	1585	425	8537	9479	26
HC_38	F	30.7	PBMCs	12750000	1530000	E	AEG,MD	1877484	366879	106835	148305	5245	22404	13883	27944	3806	323	24438	13686	10
HC_39	M	30.9	PBMCs	12600000	1512000	E	AEG,MD	640010	80488	8850	21591	1356	14618	3007	11972	658	5	8369	10062	0
HC_40	M	33.3	CD19+	31800000	680000	C	Mix I	437659	55698	10944	30331	1559	6777	2617	1390	993	55	811	220	1
HC_41	F	33.7	PBMCs	69000000	1380000	E	AEG,MD	1786984	132252	69315	31741	8289	9100	4499	2946	595	52	4578	1134	3
HC_42	F	33.8	CD19+	100000000	3360000	C	AEG,MD	1032835	195330	28072	121411	2521	23779	6294	3445	1021	139	4069	4566	13
HC_43	F	34.0	PBMCs	3000000	123000	C	AEG,MD	1598313	97235	42852	38597	2734	5965	2844	1067	336	49	2136	636	19
HC_44	M	35.3	PBMCs	15000000	1800000	E	Mix I	4584690	303597	43302	86951	11700	117932	19339	7425	3176	94	7750	5926	2
HC_45	M	35.7	PBMCs	6480000	777600	E	AEG,MD	943459	124374	24273	36725	12340	38562	3062	4235	701	37	3080	1359	0
HC_46	F	36.3	PBMCs	21600000	1300000	E	AEG,MD	1833493	187445	53829	67615	5050	20383	7927	16069	982	224	10156	5193	17
HC_47	M	39.3	PBMCs	51000000	6120000	E	Mix I	454024	47055	5645	17603	1553	14413	3212	1697	701	17	1230	968	16
HC_48	M	41.4	PBMCs	16500000	1980000	E	AEG,MD	903117	110233	32876	32955	10024	20751	2524	6928	640	5	2326	1204	0
HC_49	M	42.6	PBMCs	5700000	684000	E	AEG,MD	878951	86541	26443	42918	1667	7504	2296	2206	360	49	2121	947	30
HC_50	M	42.7	PBMCs	10000000	1200000	E	AEG,MD	1668134	69380	6353	31589	611	8976	3172	3722	1135	78	9926	3805	13
HC_51	F	45.3	PBMCs	8400000	1008000	E	AEG,MD	1445580	168554	16932	37464	6789	43558	9925	27511	1502	143	16832	7879	19
HC_52	F	45.4	PBMCs	13200000	1580000	E	AEG,MD	1694914	261324	80587	85933	15323	37856	9798	8977	4003	316	11782	6690	59
HC_53	F	50.7	PBMCs	9600000	1152000	E	AEG,MD	1970119	116853	15337	26192	8018	32846	15563	4098	1241	47	8088	5414	9

Supplementary table 2

Primer	Sequence
CHA_70x	GTGACTGGAGTTCAGACGTGTGCTCTTCCGATCTNNNNTNNNNTNNNNGAYGACCACGTTCCCATC*T
CHM_70x	GTGACTGGAGTTCAGACGTGTGCTCTTCCGATCTNNNNTNNNNTNNNNTCGTATCCGACGGGGAATT*C
CHD_70x	GTGACTGGAGTTCAGACGTGTGCTCTTCCGATCTNNNNTNNNNTNNNNGGGCTGTTATCCTTTGGGT*G
CHE_70x	GTGACTGGAGTTCAGACGTGTGCTCTTCCGATCTNNNNTNNNNTNNNNAGAGTCACGGAGGTGGCAT*T
CHG_70x	GTGACTGGAGTTCAGACGTGTGCTCTTCCGATCTNNNNTNNNNTNNNNAGTAGTCCTTGACCAGGCA*G
IGHV1_50x	ACACTCTTTCCCTACACGACGCTCTTCCGATCTGGCCTCAGTGAAGGTCTCCTGCAA*G
IGHV2_50x	ACACTCTTTCCCTACACGACGCTCTTCCGATCTGTCTGGTCCTACGCTGGTGAAACC*C
IGHV3_50x	ACACTCTTTCCCTACACGACGCTCTTCCGATCTCTGGGGGGTCCCTGAGACTCTCCT*G
IGHV4_50x	ACACTCTTTCCCTACACGACGCTCTTCCGATCTCTTCGGAGACCCTGTCCCTCACCT*G
IGHV5_50x	ACACTCTTTCCCTACACGACGCTCTTCCGATCTCGGGGAGTCTCTGAACATCTCCTG*T
IGHV6_50x	ACACTCTTTCCCTACACGACGCTCTTCCGATCTTCGCAGACCCTCTCACTCACCTGT*G
PCR1_rev	CTAGCCTTCTCGTGTGCAGACTTGAGGTCAGTG
AD50x_i1	AATGATACGGCGACCACCGAGATCTACACTATAGCCTACACTCTTTCCCTACACGACGCTCTTCCGATC*T
AD50x_i2	AATGATACGGCGACCACCGAGATCTACACATAGAGGCACACTCTTTCCCTACACGACGCTCTTCCGATC*T
AD50x_i3	AATGATACGGCGACCACCGAGATCTACACCCTATCCTACACTCTTTCCCTACACGACGCTCTTCCGATC*T
AD50x_i4	AATGATACGGCGACCACCGAGATCTACACGGCTCTGAACACTCTTTCCCTACACGACGCTCTTCCGATC*T
AD50x_i5	AATGATACGGCGACCACCGAGATCTACACAGGCGAAGACACTCTTTCCCTACACGACGCTCTTCCGATC*T
AD50x_i6	AATGATACGGCGACCACCGAGATCTACACTAATCTTAACACTCTTTCCCTACACGACGCTCTTCCGATC*T
AD50x_i7	AATGATACGGCGACCACCGAGATCTACACCAGGACGTACACTCTTTCCCTACACGACGCTCTTCCGATC*T
AD50x_i8	AATGATACGGCGACCACCGAGATCTACACGTACTGACACACTCTTTCCCTACACGACGCTCTTCCGATC*T
AD70x_i1	CAAGCAGAAGACGGCATACGAGATCGAGTAATGTGACTGGAGTTCAGACGTGTGCTCTTCCGAT*C
AD70x_i2	CAAGCAGAAGACGGCATACGAGATTCTCCGGAGTGACTGGAGTTCAGACGTGTGCTCTTCCGAT*C
AD70x_i3	CAAGCAGAAGACGGCATACGAGATAATGAGCGGTGACTGGAGTTCAGACGTGTGCTCTTCCGAT*C
AD70x_i4	CAAGCAGAAGACGGCATACGAGATGGAATCTCGTGACTGGAGTTCAGACGTGTGCTCTTCCGAT*C
AD70x_i5	CAAGCAGAAGACGGCATACGAGATTTCTGAATGTGACTGGAGTTCAGACGTGTGCTCTTCCGAT*C
AD70x_i6	CAAGCAGAAGACGGCATACGAGATACGAATTCGTGACTGGAGTTCAGACGTGTGCTCTTCCGAT*C
AD70x_i7	CAAGCAGAAGACGGCATACGAGATAGCTTCAGGTGACTGGAGTTCAGACGTGTGCTCTTCCGAT*C
AD70x_i8	CAAGCAGAAGACGGCATACGAGATGCGCATTAGTGACTGGAGTTCAGACGTGTGCTCTTCCGAT*C
AD70x_i9	CAAGCAGAAGACGGCATACGAGATCATAGCCGGTGACTGGAGTTCAGACGTGTGCTCTTCCGAT*C
AD70x_i10	CAAGCAGAAGACGGCATACGAGATTTCGCGGAGTGACTGGAGTTCAGACGTGTGCTCTTCCGAT*C
AD70x_i11	CAAGCAGAAGACGGCATACGAGATGCGCGAGAGTGACTGGAGTTCAGACGTGTGCTCTTCCGAT*C
AD70x_i12	CAAGCAGAAGACGGCATACGAGATCTATCGCTGTGACTGGAGTTCAGACGTGTGCTCTTCCGAT*C

Reverse Transcription

Primers_mix	MD mix		AEG mix			Mix I					
Primers	CHM_70x	CHD_70x	CHA_70x	CHE_70x	CHG_70x	CHM_70x	CHD_70x	CHA_70x	CHE_70x	CHG_70x	Total
Concentration (uM)	0.625	0.625	0.25	0.25	0.75	0.03125	0.03125	0.0625	0.125	1	1.25

PCR1

Primers	IGHV1_50x	IGHV2_50x	IGHV3_50x	IGHV4_50x	IGHV5_50x	IGHV6_50x	PCR1_rev	Total
Concentration (uM)	1.25						1.25	2.5

PCR2

Primer	AD70x	AD50x	Total
Concentration (uM)	1.25	1.25	2.5